

AD-750 590

A LAPLACE TRANSFORM AMPLITUDE FUNCTION
GENERATOR UTILIZING A THIN FILM SEMI-
CONDUCTOR

James E. Brown, Jr.

Army Missile Command
Redstone Arsenal, Alabama

31 July 1972

DISTRIBUTED BY:

NTIS

National Technical Information Service
U. S. DEPARTMENT OF COMMERCE
5285 Port Royal Road, Springfield Va. 22151

AD

AD 750590

REPORT NO. RC-TR-72-2

A LAPLACE TRANSFORM AMPLITUDE FUNCTION GENERATOR
UTILIZING A THIN FILM SEMICONDUCTOR

by

James E. Brown, Jr.

July 1972

APPROVED FOR PUBLIC RELEASE; DISTRIBUTION UNLIMITED.



U.S. ARMY MISSILE COMMAND

Redstone Arsenal, Alabama

NATIONAL TECHNICAL
INFORMATION SERVICE

D D C
RECEIVED
NOV 8 1972
RECEIVED
B

DISPOSITION INSTRUCTIONS

DESTROY THIS REPORT WHEN IT IS NO LONGER NEEDED. DO NOT RETURN IT TO THE ORIGINATOR.

APPROVED FOR	
DATE	BY
BY	
DISTRIBUTION/AVAILABILITY CODES	
DOW. Avail. and/or SPECIAL	
A	

DISCLAIMER

THE FINDINGS IN THIS REPORT ARE NOT TO BE CONSTRUED AS AN OFFICIAL DEPARTMENT OF THE ARMY POSITION UNLESS SO DESIGNATED BY OTHER AUTHORIZED DOCUMENTS.

TRADE NAMES

USE OF TRADE NAMES OR MANUFACTURERS IN THIS REPORT DOES NOT CONSTITUTE AN OFFICIAL INDORSEMENT OR APPROVAL OF THE USE OF SUCH COMMERCIAL HARDWARE OR SOFTWARE.

UNCLASSIFIED
Security Classification

DOCUMENT CONTROL DATA - R & D

(Security classification of title, body of abstract and indexing annotation must be entered when the original report is classified)

1. ORIGINATING ACTIVITY (Corporate author) Systems Engineering & Integration Office Directorate for Res, Dev, Eng & Mal Sys Lab US Army Missile Command Redstone Arsenal, Alabama 35809		2a. REPORT SECURITY CLASSIFICATION UNCLASSIFIED	
		2b. GROUP NA	
3. REPORT TITLE A LAPLACE TRANSFORM AMPLITUDE FUNCTION GENERATOR UTILIZING A THIN FILM CONDUCTOR			
4. DESCRIPTIVE NOTES (Type of report and inclusive dates) Technical Report			
5. AUTHOR(S) (First name, middle initial, last name) James E. Brown, Jr.			
6. REPORT DATE 31 July 1972		7a. TOTAL NO. OF PAGES 74 80	7b. NO. OF REFS 7
8a. CONTRACT OR GRANT NO.		8b. ORIGINATOR'S REPORT NUMBER(S) RC-TR-72-2	
a. PROJECT NO. NA		8d. OTHER REPORT NO(S) (Any other numbers that may be assigned this report) AD _____	
10. DISTRIBUTION STATEMENT Approved for public release; distribution unlimited.			
11. SUPPLEMENTARY NOTES None		12. SPONSORING MILITARY ACTIVITY Same as No. 1	
13. ABSTRACT The characteristics of man's systems can be predetermined by application of an analog. This report was developed to produce a better tool in the area of the electric field analog. It develops as a straightforward proof of the analog existence with the main body being experimental. The experimental area develops in normal form with early familiarization methods through various phases to the final result. The semiconductor can be used with more consistency, and better results, than any present guaranteed device on the market. Details of illustrations in this document may be better studied on microfiche			

DD FORM 1473
NOV 68

REPLACES DD FORM 1473, 1 JAN 63, WHICH IS OBSOLETE FOR ARMY USE.

UNCLASSIFIED
Security Classification

I H

14. KEY WORDS	LINK A		LINK B		LINK C	
	ROLE	WT	ROLE	WT	ROLE	WT
Laplace transform amplitude function generator Thin film semiconductor Semiconductor wafers						

I-B

31 July 1972

Report No. RC-TR-72-2

A LAPLACE TRANSFORM AMPLITUDE FUNCTION GENERATOR
UTILIZING A THIN FILM CONDUCTOR

by

James E. Brown, Jr.

APPROVED FOR PUBLIC RELEASE; DISTRIBUTION UNLIMITED.

Systems Engineering and Integration Office
Directorate for Research, Development, Engineering
and Missile Systems Laboratory
US Army Missile Command
Redstone Arsenal, Alabama 35809

I-C

ABSTRACT

The characteristics of many systems can be predetermined by application of an analog. This report was developed to produce a better tool in the area of the electric field analog. It develops as a straightforward proof of the analog existence with the main body being experimental. The experimental area develops in normal form with early familiarization methods through various phases to the final result. The semiconductor can be used with more consistency, and better results, than any present guaranteed device on the market.

ACKNOWLEDGMENT

Appreciation is expressed to Dr. Eugene C. Huebschmann and others of the University of Tennessee Space Institute for their technical advice and direction throughout this study. Appreciation is expressed to the United States Government through the US Army Missile Command for the opportunity to engage in this endeavor. Appreciation for the advice on and construction of the semiconductor wafers is expressed to the semiconductor facility personnel of the Astrionics Laboratory of the Marshall Space Flight Center.

CONTENTS

CHAPTER	PAGE
I. INTRODUCTION	1
II. DEVELOPMENT OF THE POTENTIAL ANALOG	5
III. PHYSICAL CONSIDERATIONS	22
IV. EXPERIMENTAL PROCEDURE AND RESULTS	27
Resistance Experiments	27
Linearity Experiments	33
Contact and Function Experiments	43
Function Generator Experiments	55
V. RESULTS AND CONCLUSIONS	67
BIBLIOGRAPHY	71

LIST OF SYMBOLS

d	Radial distance from center contact to measured point on a wafer
E	Voltage applied to wafer center contact
E_a	Actual voltage at a measured point
E_m	Measured voltage
G	Network transfer function
K_D	Wafer contact separation per frequency unit
K_1	Constant to calculate a logarithm curve from experimental data
K_2	Scale factor relating Laplace function to experimental data
K_3	Scale factor relating the experimental voltage reference to the Laplace function
m	Distance between wafer contacts
p	Pole in the X function and s plane
r	Zero in the X function and s plane
U	Real component of W
V	Imaginary component of W
\bar{W}	Force exerted by λ on a unit charge in the Z plane
Z	Complex function made up of x and y . Also used to define the plane containing x and y
α	Angle related to r
β	Angle related to p
ϵ	Relative dielectric constant
ϵ_0	Permittivity of free space

- θ Angle of \bar{W} relative to the x axis in Z
- λ Charge at the center of the Z plane
- ϕ Equipotential lines
- χ Work required to move a charge in the Z plane
- ψ Streamlines

CHAPTER I

INTRODUCTION

The evolution of modern technology over the past three decades has been made possible by the development of computation and simulation capability. The first devices to be used on a large scale were primarily those of an analog type. The drift and source power sensitivities were accepted and compensated for with either manual calculation or adjustment.

As the decade of the fifties evolved, the digital computer became of age from the clumsy tube, drum memory, neat cooler container type of the 1950 vintage to the transistor discrete component type of the 1960 period.

The present mechanization in the digital and analog circuit area is the semiconductor integrated circuit unit. The area of simulation has moved to the combining of analog and digital techniques in the "hybrid configuration."

With the advent of this type of operation, the ready transfer from one technique to another on a real time basis becomes necessary. Many of the present thin sheet analog devices are impractical to automate while others require a complete servo system to generate the necessary functions. The purpose of this report is to investigate one possible method to alleviate this situation.

It should be remembered throughout this report that the thin film analogy has been used for a number of applications. The requirements

for homogeneous, uniform, and isotropic material together with accurate contact take-off are universal and not limited to the discussion of a particular function.

This has been pointed out by Reynolds in his thesis [1]¹ and amplified in a number of discussions and papers by Huebschmann [2]. While Reynolds dealt with the analog in great detail and indicated the application to function generation, the primary purpose of this report is to investigate a method rather than prove application in all facets as an analog.

According to Karplus [3], the first conductive sheet was demonstrated by Kirchoff in 1845 and utilized copper. A number of metallized type devices have been developed for various products. In 1875 an electrolyte was utilized for development of various models which was dominant until the development of Teledeltos paper in 1948. There were some successful developments before Teledeltos; one of the most notable was Kayan's [4] use of metallic conductive sheets.

The use of low-resistivity metallic sheets presents one limit of the application which requires reading of potentials to a high degree of accuracy. This probably accounts for the low level of application until the development of Teledeltos paper.

The Teledeltos paper has been widely used despite the fact that it has poor characteristics for the application. It is susceptible to puncture with the probe pressure and to tear with application of

¹Numbers in brackets refer to similarly numbered references in the bibliography.

stress. It can however be purchased reasonably cheap and the widths of approximately 3 feet help to resolve the problems of an "infinite" sheet. Teledeltos paper was used for investigation in a report by Huebschmann and Pender [2] in 1970 together with other materials. This report essentially verified findings as to shortcomings for the application.

Thin conductive sheets have been used as analogues to determine behavior in a number of fields related to physical phenomena. The materials used as discussed have varied in type and apparatus mechanization in a number of ways. Previous investigations by ICING Research Staff [5] in 1953 indicate that resistivity ranges from 100 to 100,000 ohms per square are suitable for this application. The errors in utilization of this technique can be separated; this report deals with a number of these.

The uniformity throughout a particular sheet of material and the location accuracy of source, sink, and measurement points are of primary concern. This report deals with the possibility of utilizing a semiconductor wafer with its uniform conductivity and with micro-circuit location accuracy for application to the problem.

The primary advantage of using the semiconductor thin film together with possible deposition of contacts, if accuracy requirements can be met, is in the area of minimum cost units which possibly could be stacked and switched to generate any desirable function. Electronic switching could provide a hybrid interface for use with digital machines where application of the analog becomes the most efficient method of investigation.

A brief discussion of the electric field with the final form of its potential function will be developed simultaneously with a corresponding Laplace equation to prove the validity of the analogy.

A discussion of various units now in existence together with their size, cost, and accuracy data will be furnished and a comparison will be made as to what might be expected from use of semiconductor sheets.

A chapter will be devoted to experiments which have been made to investigate the application and limitations and phenomena which were observed. A final discussion will be furnished on conclusions which can be drawn from this work and a method will be suggested for further pursuit or discard of the approach.

CHAPTER II

DEVELOPMENT OF THE POTENTIAL ANALOG

In discussing the potential analogy dealt with in this report, a cursory review of the complex potential area is adequate. To review the complex potential and indicate validity of the mathematical approach, a limited review in a narrow area of complex variables is a necessity. Consideration of the complex variable theory will be inserted at various points throughout the discussion for the purpose of continuity. The section will be developed by establishing the equation for an infinite sheet and showing it to be identical to the investigated devices.

Chen [6] presents a more detailed discussion than that presented in this study and is the primary reference for this work.

If we place an infinitely long line through the origin of the Z plane, Figure 1, and define the charge on it as λ along the length of line, it will produce an electric field in the Z plane.

We define \bar{W} as the force on a unit charge, of the same polarity as the line, due to λ . This by definition becomes the electric field intensity of charge λ .

The magnitude of this force is known to be

$$|\bar{W}| = \frac{\lambda}{2 \pi \epsilon |Z|}$$

where Z is the distance from the line charge in meters, ϵ is the relative dielectric constant,

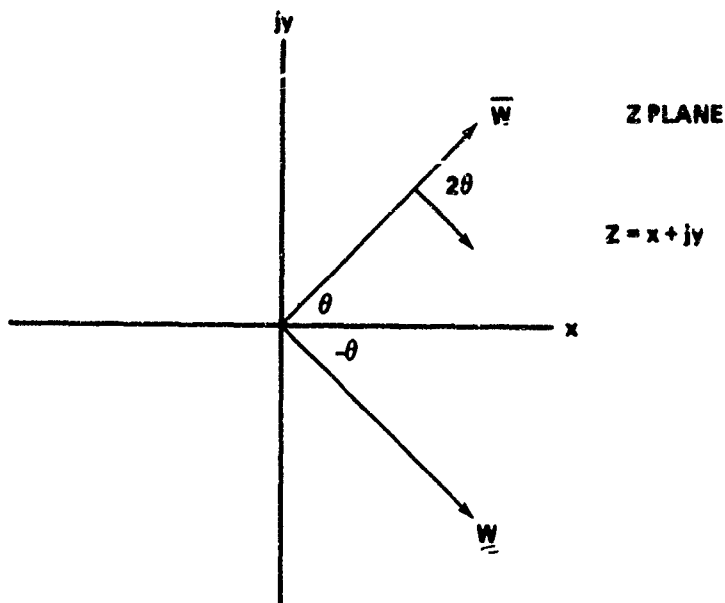


Figure 1. Line charge in the Z plane.

$$\epsilon_0 = \frac{10^7}{4\pi C^2} \quad , \quad \text{and}$$

$|\bar{W}|$ is in newtons.

Because the force is along a direction of the vector in Figure 1, we can specify

$$\bar{W} = |\bar{W}| \underline{\ell} = \frac{\lambda}{2\pi\epsilon|Z|} \underline{\ell}$$

but,

$$\underline{\ell} = 1 \underline{\ell} = \frac{|Z|}{|Z|} \underline{\ell} = \frac{Z}{|Z|}$$

and

$$\bar{W} = \frac{\lambda Z}{2\pi\epsilon|Z|^2} \quad ;$$

however.

$$|z|^2 = z \bar{z}$$

where \bar{z} = complex conjugate of z , and

$$\bar{W} = \frac{\lambda}{2\pi\epsilon\bar{z}}, \quad (1)$$

which represents the actual electric field due to λ . The conjugate

$$W = \frac{\lambda}{2\pi\epsilon z} \quad (2)$$

At this point it is necessary to investigate these two functions considered as complex variables.

We consider

$$W = f(z)$$

$$z = x + jy$$

$$W = U + jV = f(x + jy),$$

then

$$U = U(x, y)$$

$$V = V(x, y).$$

From this,

$$\begin{aligned} W = \frac{1}{z} &= \frac{1}{x + jy} \frac{(x - jy)}{(x - jy)} \\ &= \frac{x}{x^2 + y^2} + \frac{j(-y)}{x^2 + y^2} \end{aligned}$$

$$U = \frac{x}{x^2 + y^2} \quad (3)$$

$$V = \frac{-y}{x^2 + y^2} \quad (4)$$

This procedure is used to determine relationships to analyticity of the two functions in Z and hence the following definition.

A function is analytic throughout a region R of the Z plane if its derivative dW/dZ exists at every point in the region and the function is single valued throughout R.

Define

$$\frac{dW}{dZ} = \lim_{\Delta Z \rightarrow 0} \frac{\Delta W}{\Delta Z}$$

There is more than one way to let $\Delta Z \rightarrow 0$. If we consider $\Delta y \rightarrow 0$ initially, then

$$\frac{dW}{dZ} = \lim_{\Delta x \rightarrow 0} \frac{\Delta W}{\Delta x + 0} = \frac{\partial W}{\partial x}$$

or if $\Delta x \rightarrow 0$ initially,

$$\frac{dW}{dZ} = \lim_{\Delta y \rightarrow 0} \frac{W}{0 + j\Delta y} = \frac{1}{j} \frac{\partial W}{\partial y}$$

If the derivative dW/dZ exists at any point, it must have a unique value at that point independent of the direction of approach. Hence for a derivative to exist

$$\frac{\partial W}{\partial x} = \frac{1}{j} \frac{\partial W}{\partial y}$$

but

$$\frac{\alpha \bar{W}}{\alpha x} = \frac{\alpha U}{\alpha x} + j \frac{\alpha V}{\alpha x}$$

and

$$\frac{1}{j} \frac{\alpha \bar{W}}{\alpha y} = \frac{\alpha V}{\alpha y} - j \frac{\alpha U}{\alpha y}$$

from which

$$\frac{\alpha U}{\alpha x} = \frac{\alpha V}{\alpha y} \quad (5)$$

$$\frac{\alpha U}{\alpha y} = - \frac{\alpha V}{\alpha x} \quad (6)$$

These Cauchy-Reimann equations are normally considered necessary but not sufficient conditions to guarantee the existence of a derivative. In this work, however, Equation (5) or Equation (6) can be considered as sufficient.

We can now investigate:

$$\bar{W} = \frac{1}{z} = \frac{1}{x - jy} \frac{(x + jy)}{(x + jy)} = \frac{x}{x^2 + y^2} + j \frac{y}{x^2 + y^2}$$

$$\bar{W} = U + jV$$

$$U = \frac{x}{x^2 + y^2}$$

$$\frac{\alpha U}{\alpha y} = \frac{-2xy}{(x^2 + y^2)^2}$$

$$\frac{\alpha U}{\alpha x} = \frac{y^2 - x^2}{(x^2 - y^2)^2}$$

and

$$v = \frac{y}{x^2 + y^2}$$

$$\frac{\partial v}{\partial y} = \frac{x^2 - y^2}{(x^2 + y^2)^2}$$

$$\frac{\partial v}{\partial x} = \frac{-2xy}{(x^2 + y^2)^2}$$

Neither of the Cauchy-Reimann equations hold and therefore $1/\bar{z}$ is not analytic. From Equations (3) and (4) for $W = 1/z$,

$$U = \frac{x}{x^2 + y^2}$$

$$\frac{\partial U}{\partial y} = \frac{-2xy}{(x^2 + y^2)^2}$$

$$\frac{\partial U}{\partial x} = \frac{y^2 - x^2}{(x^2 + y^2)^2}$$

$$v = \frac{-y}{x^2 + y^2}$$

$$\frac{\partial v}{\partial y} = \frac{y^2 - x^2}{(x^2 + y^2)^2} \quad \frac{\partial v}{\partial x} = \frac{2xy}{(x^2 + y^2)^2}$$

and

$$\frac{\partial U}{\partial x} = \frac{\partial v}{\partial y} \quad \frac{\partial U}{\partial y} = \frac{-\partial v}{\partial x}$$

Then $1/z$ is an analytic function which denotes analyticity at all but the functions own singular points which in this case exists at $0 + j 0$.

Let it suffice in further development of the function $W = 1/Z$, where $Z = x + jy$, to state that the integral of an analytic function also satisfies the Cauchy-Riemann equations and is analytic over the specified region.

Figure 2 illustrates the movement of a unit charge a distance of dZ over the path Z_0, Z . From Equation (2) the force at Z is

$$W = \frac{\lambda}{2\pi\epsilon Z}$$

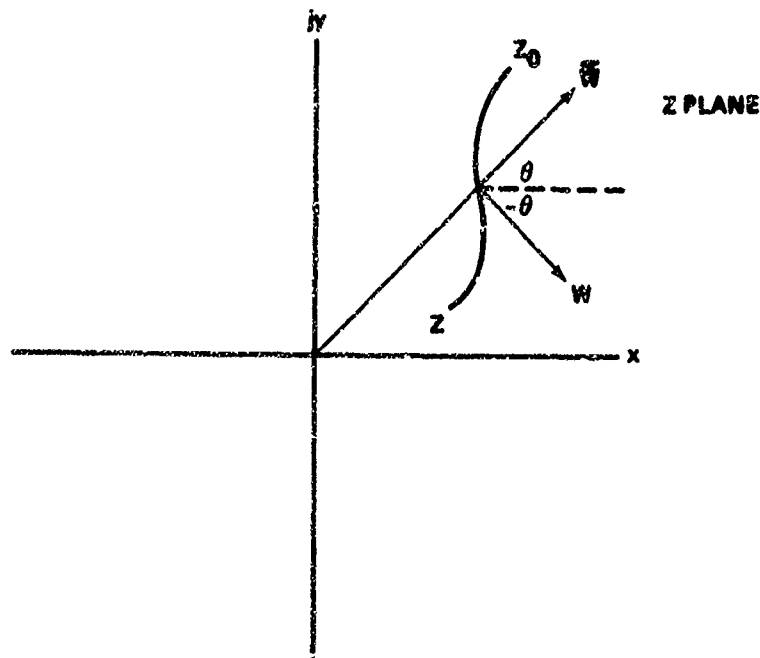


Figure 2. Force components in the Z plane.

Since we are moving counter to the force or field intensity a distance of dZ , the work or complex potential to move over the path Z_0 to Z is

$$\begin{aligned}
\chi(Z) &= \int_{Z_0}^Z -W(Z) dz = \int_{Z_0}^Z \frac{-\lambda}{2\pi\epsilon Z} dz \\
&= \frac{-\lambda}{2\pi\epsilon} (\ln Z + \ln Z_0) \\
&= \frac{-\lambda}{2\pi\epsilon} \ln \frac{Z}{Z_0} .
\end{aligned}$$

We can choose Z_0 as a reference point of 1 or the point where $\chi(Z_0) = 0$, then

$$\begin{aligned}
\chi(Z) &= \frac{-\lambda}{2\pi\epsilon} \ln Z \\
&= \frac{-\lambda}{2\pi\epsilon} \ln |Z| e^{j\theta}
\end{aligned}$$

$$\chi(Z) = \theta(x, y) = \phi(x, y) + j\psi(x, y) \quad (7)$$

$$\phi = \frac{-\lambda}{2\pi\epsilon} \ln |Z| = \text{equipotential} \quad (8)$$

$$\psi = \frac{-\lambda}{2\pi\epsilon} e^{j\theta} = \text{streamline} \quad (9)$$

Figure 3 presents a plot in the Z plane of Equations (8) and (9) with various $|Z|$ and θ held constant. It can be seen that Equation (8) represents equal potential lines at radius equal to $|Z|$. Because Z_0 was chosen equal to 1, measurements from that point for $|Z| < |Z_0|$ can be considered positive potential lines and those with $|Z| > |Z_0|$ as negative potential contours. The manipulation of $Z_0 = 1$ implies $Z_0 = 1/\theta$ and hence ψ would be referenced from a given angle, in this case chosen as the positive x . The $j\psi(x, y)$ in Equation (7) as compared to $\phi(x, y)$ indicates the orthogonality of the streamlines and equipotentials.

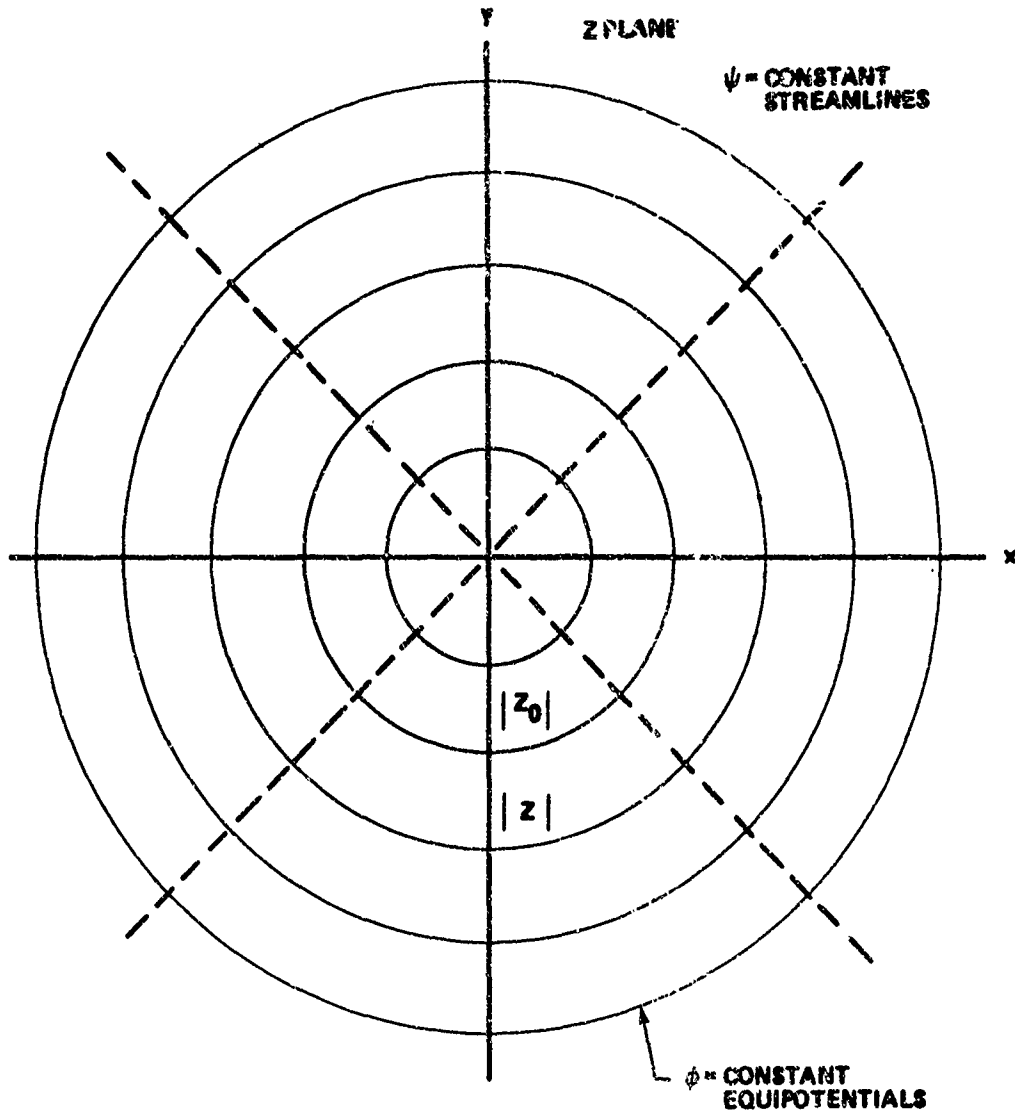


Figure 3. Electric field plot with equipotentials and streamlines.

For a single positive line charge at $P = x_p + jy_p$, the substitution $Z = Z - p$ can be made and

$$\chi(Z') = \frac{\lambda}{2\pi\epsilon} \ln \frac{1}{Z'} + \frac{\lambda}{2\pi\epsilon} \ln Z'_0$$

$$\chi(Z) = \frac{\lambda}{2\pi\epsilon} \ln \frac{1}{Z - p} + \frac{\lambda}{2\pi\epsilon} \ln (Z_0 - p)$$

Because

$$-W = -(W_1 + W_2 + \dots + W_n)$$

for several line charges of mixed polarity and equal value in the Z plane,

$$\chi(Z) = \frac{\lambda}{2\pi\epsilon} \ln \frac{(Z - r_1)(Z - r_2) \dots (Z - r_m)}{(Z - p_1)(Z - p_2) \dots (Z - p_m)} + C \quad (10)$$

with

$$C = -\frac{\lambda}{2\pi\epsilon} \ln \frac{(-r_1)(-r_2) \dots (-r_m)}{(-p_1)(-p_2) \dots (-p_m)} \quad (10a)$$

where $Z_0 = 0$.

Equation (10) can be written where $Z - r$ is a complex $\phi(x, y) + j\psi(x, y)$ and

$$z - r_1 = |z - r_1| e^{\alpha_1}$$

$$z - r_2 = |z - r_2| e^{\alpha_2}$$

.

.

.

$$z - r_m = |z - r_m| e^{\alpha_m}$$

$$z - p_1 = |z - p_1| e^{\beta_1}$$

$$z - p_2 = |z - p_2| e^{\beta_2}$$

.

.

.

$$z - p_n = |z - p_n| e^{\beta_n}$$

$$\begin{aligned} \chi(z) = & \frac{\lambda}{2\pi\epsilon} \left(\ln|z - r_1| + \ln|z - r_2| + \dots + \ln|z - r_m| \right. \\ & \left. - \ln|z - p_1| - \ln|z - p_2| - \dots - \ln|z - p_n| \right) \\ & - \frac{\lambda}{2\pi\epsilon} \left(\ln|r_1| + \ln|r_2| + \dots + \ln|r_m| - \ln|p_1| \right. \\ & \left. - \ln|p_2| - \dots - \ln|p_n| \right) \\ & + \frac{\lambda}{2\pi\epsilon} \left(\alpha_1 + \alpha_2 + \dots + \alpha_m - \beta_1 - \beta_2 - \dots - \beta_n + r \right) \quad (11) \end{aligned}$$

where $r =$ summation of all angles in C .

Equations (10), (10a), and (11) are the equations for the electric potential function in an infinite thin plane with mixed polarity charges at various locations in the plane.

It now remains to investigate the development of Laplace transforms and their final form to insure that Equations (10), (10a), and (11) are indeed a sufficient analogue. To evaluate the usefulness of the transform, let us consider the type of systems for which it can be utilized. This is intended as a cursory look at the subject sufficient to justify the approach in this report. There is excellent text on the subject complete with tables of the transforms.

Let us state that the Laplace transform can be used in the solution of linear differential equations and these in turn reflect most of the physical networks and systems with which we deal. Let the statement stand that by definition a linear system is one for which superposition is valid and that the response to a sum of inputs is equal to the sum of the response of the inputs applied separately.

If we have a differential equation of the form:

$$A_0(x) \frac{d^2 y}{dx^2} + A_1(x) \frac{dy}{dx} + A_2(x) y = f_1(x)$$

and letting $y_1(x)$ and $y_2(x)$ represent solutions then

$$\begin{aligned} A_0(x) \frac{d^2(y_1 + y_2)}{dx^2} + A_1(x) \frac{d(y_1 + y_2)}{dx} + A_2(x)(y_1 + y_2) \\ = f_1(x) + f_2(x) \end{aligned}$$

The classical solution of this type equation is well known; however, the Laplace transform offers a number of advantages such as algebraic solutions together with established tables which make the solution simpler.

The Laplace transform for a function of $f(t)$ is defined by

$$L[f(t)] = \int_0^{\infty} f(t) e^{-st} dt = F(s) \quad .$$

As an example, to transform $\sin Bt$:

$$\begin{aligned} L \sin Bt &= \int_0^{\infty} \frac{e^{iBt} - e^{-iBt}}{2i} e^{-st} dt \\ &= \frac{1}{2i} \int_0^{\infty} e^{iBt} e^{-st} dt - \int_0^{\infty} e^{-iBt} e^{-st} dt \\ &= \frac{1}{2i} \left[\frac{e^{(iB - s)t}}{iB - s} \Big|_0^{\infty} - \frac{e^{-(iB + s)t}}{iB + s} \Big|_0^{\infty} \right] \\ &= \frac{1}{2i} \left[-\frac{1}{iB - s} - \frac{i}{iB + s} \right] \\ &= \frac{B}{B^2 + s^2} \quad . \end{aligned}$$

To deal with electric networks, we could look at transforms of operations:

$$L\left[\frac{df}{dt}\right] = \int_0^{\infty} \frac{df}{dt} e^{-st} dt$$

by letting

$$u = e^{-st}$$

and

$$dv = \frac{df}{dt} dt$$

then

$$\int_0^{\infty} \frac{df}{dt} e^{-st} dt = f(t) e^{-st} \Big|_0^{\infty} + s \int_0^{\infty} f(t) e^{-st} dt$$

and

$$L\left[\frac{df}{dt}\right] = -f(0) + s f(s)$$

where

$$\lim_{t \rightarrow \infty} f(t) e^{-st} = 0$$

$$L\left[\int_0^t f(x) dx\right] = \int_0^{\infty} e^{-st} dt \int_0^t f(x) dx$$

by letting

$$u = \int_0^t f(x) dx,$$

$$du = f(t) dt,$$

$$v = -\frac{1}{s} e^{-st},$$

and

$$dv = e^{-st} dt$$

then

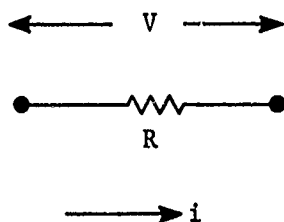
$$\int_0^{\infty} e^{-st} dt \int_0^t f(x) dx = -\frac{1}{s} e^{-st} \int_0^t f(x) dx + \frac{1}{s} \int_0^{\infty} e^{-st} f(t) dt$$

and

$$L \left[\int_0^t f(x) dx \right] = 0 + \frac{1}{s} \int_0^{\infty} e^{-st} f(t) dt = \frac{F(s)}{s}$$

These transforms are sufficient to allow investigation of electrical elements and consequent development of a network transfer function.

Let us first consider a resistor:



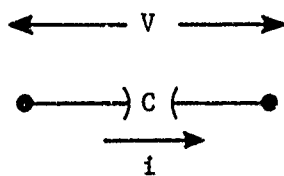
$$v = Ri$$

$$i = \frac{v}{R}$$

$$V(S) = RI(S)$$

$$I(S) = \frac{V(S)}{R}$$

For a capacitor:



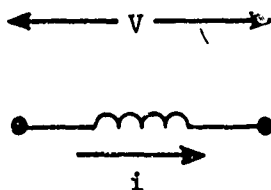
$$V = \frac{1}{C} \int_0^t i \, dt + V(0)$$

$$i = C \frac{dv}{dt}$$

$$V(S) = \frac{1}{CS} I(S) + \frac{V(0)}{S}$$

$$I(S) = CSV(S) - Cv(0)$$

and finally for an inductor:



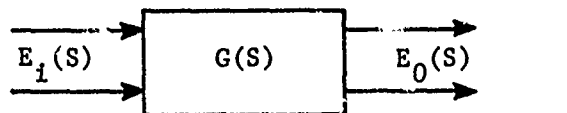
$$V = L \frac{di}{dt}$$

$$i = \frac{1}{L} \int_0^t V \, dt + i(0)$$

$$V(S) = LS I(S) - Li(0)$$

$$I(S) = \frac{1}{LS} V(S) - \frac{i(0)}{S} ..$$

If we therefore treat the relationship of an input to an output as a transfer function $G(S)$



then

$$\frac{E_0(S)}{E_1(S)} = G(S)$$

$G(S)$ is written in the form

$$G(S) = \frac{a(s - r_1)(s - r_2) \dots (s - r_n)}{b(s - p_1)(s - p_2) \dots (s - p_m)}$$

then

$$\ln|G(S)| = \ln \frac{a}{b} + \ln \frac{(S - r_1)(S - r_2) \dots (S - r_m)}{(S - p_1)(S - p_2) \dots (S - p_n)}$$

which is exactly analogous to Equation (10) where $\ln \frac{a}{b}$ is equivalent to C.

CHAPTER III

PHYSICAL CONSIDERATIONS

There are a number of physical limitations relative to use of the thin sheet analog principle as a practical tool. Since the purpose of this report is related primarily to investigation of a single method, it would do well to discuss others and relate them to various limitations. The limits to be discussed are as follows:

1. Size.
2. Material.
3. Contact Problems.
4. Mechanical Measurement Limitations.
5. Accuracy.
6. Operating Complexity.

To discuss these limitations, it is necessary to relate requirements only to an idealized surface with the simple equation of

$$E_m = E \ln d \quad (12)$$

where polarity is ignored and

E_m = measured voltage

E = applied potential at the center of an infinite sheet.

(resulting in constant current)

d = radial distance from the center point.

All of the equations developed in Chapter II were related to an infinite sheet. This is not practical and destroys the basic investigation which relates to a simple, low priced unit for general use.

If d in Equation (12) is allowed to equal Km , where m = increment of distance measurement and K = number of increments internal, and if the potential is applied at a perfect circular contact on a limited sheet at the maximum k , all internal points are a perfect representation of Equation (12). This is shown in Figure 4.

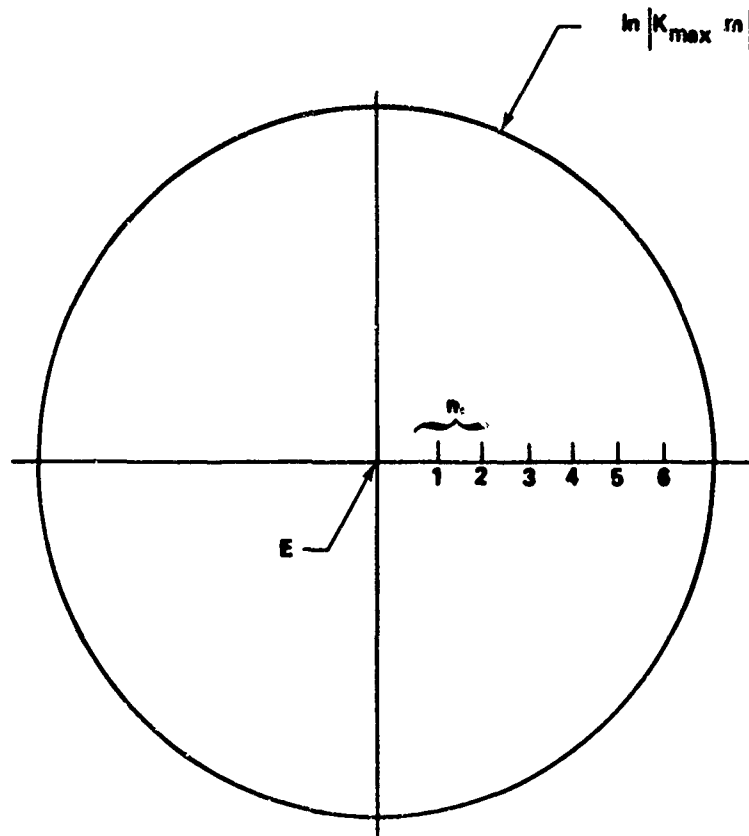


Figure 4. Equipotentials at discrete intervals.

Therefore excluding all other considerations, a circular sheet of any size with applied potentials as defined represent a perfect device in reflecting Equation (12). Other considerations limit the size to some minimum and these considerations will be discussed.

The ICING Research Staff [5] investigated a number of possible conductive materials and their findings can be summarized as follows to eliminate a number of approaches:

1. Metal foils are too low in resistivity.
2. Metallic coated conductors have unacceptable variations in space conductivity.
3. Electrolytic conductors are best applied in tanks and therefore not suitable to the problem.
4. Teledeltos paper has disadvantages (previously discussed).
5. Conductive paint has some promise but production problems are rather strenuous.

One of the most potent designs available at present is the ESIAC computer [7]. This device uses the Factor Analog method with a large carbon conductor sheet. It requires setting and manipulation of pole-zero probes and with the readout is approximately the size of a large desk. While it is an extremely useful device, it remains larger and more complex than the one being investigated.

One of the problems which becomes obvious is distortion of the field resulting from contacts with conductivity different from the film. The contacts themselves must be negligible relative to the overall area of the sheet. Measuring instrumentation input impedance must be kept large to prevent distortion. Coincident with these problems, the contact and measuring system must avoid the errors of nonpredictable large contact drop.

In a relatively large sheet system where a movable small number of contacts are utilized, the problem is not as great as one with fixed

If d in Equation (12) is allowed to equal Km , where m = increment of distance measurement and K = number of increments internal, and if the potential is applied at a perfect circular contact on a limited sheet at the maximum k , all internal points are a perfect representation of Equation (12). This is shown in Figure 4.

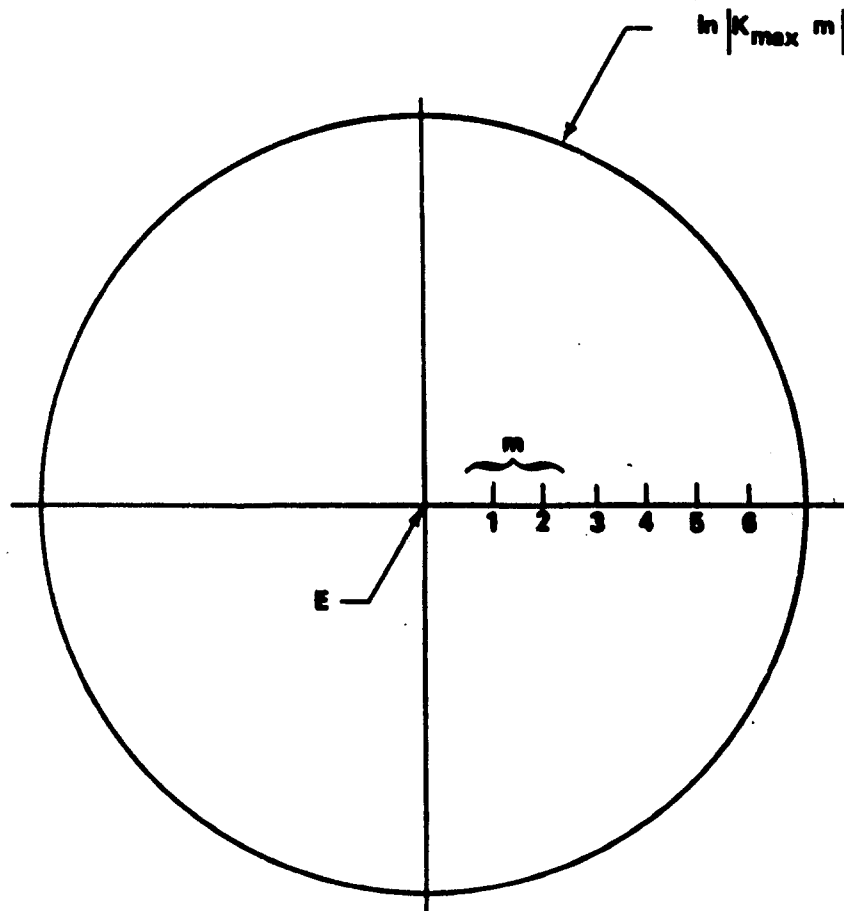


Figure 4. Equipotentials at discrete intervals.

Therefore excluding all other considerations, a circular sheet of any size with applied potentials as defined represent a perfect device in reflecting Equation (12). Other considerations limit the size to some minimum and these considerations will be discussed.

The ICING Research Staff [5] investigated a number of possible conductive materials and their findings can be summarized as follows to eliminate a number of approaches:

1. Metal foils are too low in resistivity.
2. Metallic coated conductors have unacceptable variations in space conductivity.
3. Electrolytic conductors are best applied in tanks and therefore not suitable to the problem.
4. Teledeltos paper has disadvantages (previously discussed).
5. Conductive paint has some promise but production problems are rather strenuous.

One of the most potent designs available at present is the ESIAC computer [7]. This device uses the Factor Analog method with a large carbon conductor sheet. It requires setting and manipulation of pole-zero probes and with the readout is approximately the size of a large desk. While it is an extremely useful device, it remains larger and more complex than the one being investigated.

One of the problems which becomes obvious is distortion of the field resulting from contacts with conductivity different from the film. The contacts themselves must be negligible relative to the overall area of the sheet. Measuring instrumentation input impedance must be kept large to prevent distortion. Coincident with these problems, the contact and measuring system must avoid the errors of nonpredictable large contact drop.

In a relatively large sheet system where a movable small number of contacts are utilized, the problem is not as great as one with fixed

If d in Equation (12) is allowed to equal Km , where $m =$ increment of distance measurement and $K =$ number of increments internal, and if the potential is applied at a perfect circular contact on a limited sheet at the maximum k , all internal points are a perfect representation of Equation (12). This is shown in Figure 4.

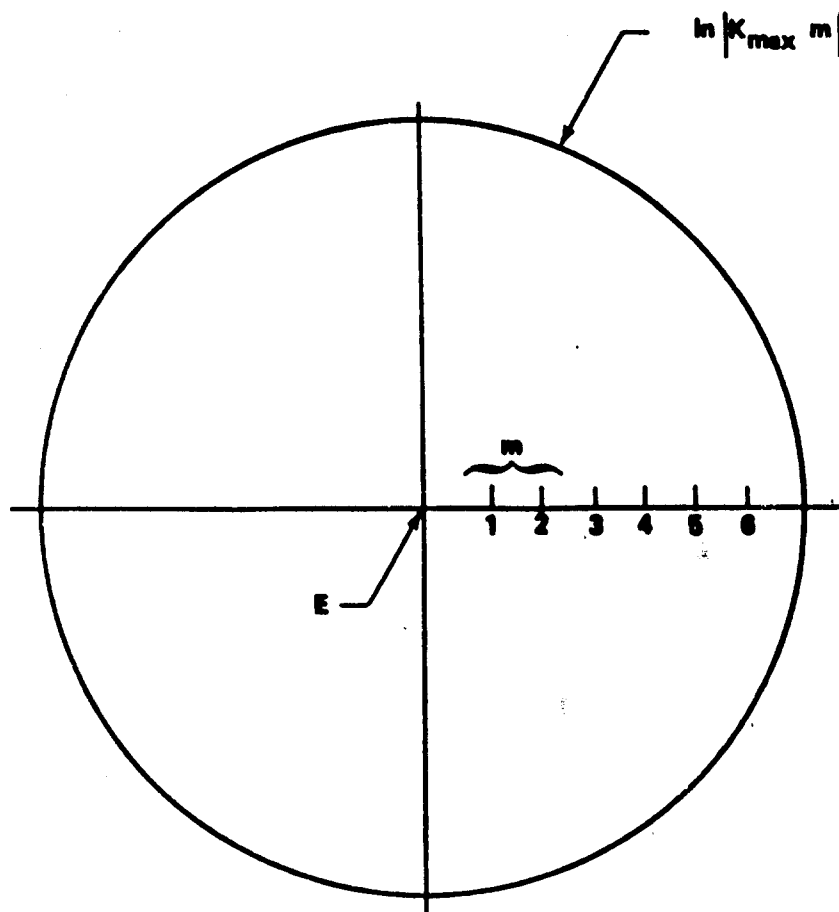


Figure 4. Equipotentials at discrete intervals.

Therefore excluding all other considerations, a circular sheet of any size with applied potentials as defined represent a perfect device in reflecting Equation (12). Other considerations limit the size to some minimum and these considerations will be discussed.

The ICINC Research Staff [5] investigated a number of possible conductive materials and their findings can be summarized as follows to eliminate a number of approaches:

1. Metal foils are too low in resistivity.
2. Metallic coated conductors have unacceptable variations in space conductivity.
3. Electrolytic conductors are best applied in tanks and therefore not suitable to the problem.
4. Teledeltos paper has disadvantages (previously discussed).
5. Conductive paint has some promise but production problems are rather strenuous.

One of the most potent designs available at present is the ESIAC computer [7]. This device uses the Factor / analog method with a large carbon conductor sheet. It requires setting and manipulation of pole-zero probes and with the readout is approximately the size of a large desk. While it is an extremely useful device, it remains larger and more complex than the one being investigated.

One of the problems which becomes obvious is distortion of the field resulting from contacts with conductivity different from the film. The contacts themselves must be negligible relative to the overall area of the sheet. Measuring instrumentation input impedance must be kept large to prevent distortion. Coincident with these problems, the contact and measuring system must avoid the errors of unpredictable large contact drop.

In a relatively large sheet system where a movable small number of contacts are utilized, the problem is not as great as one with fixed

If d in Equation (12) is allowed to equal Km , where m = increment of distance measurement and K = number of increments internal, and if the potential is applied at a perfect circular contact on a limited sheet at the maximum k , all internal points are a perfect representation of Equation (12). This is shown in Figure 4.

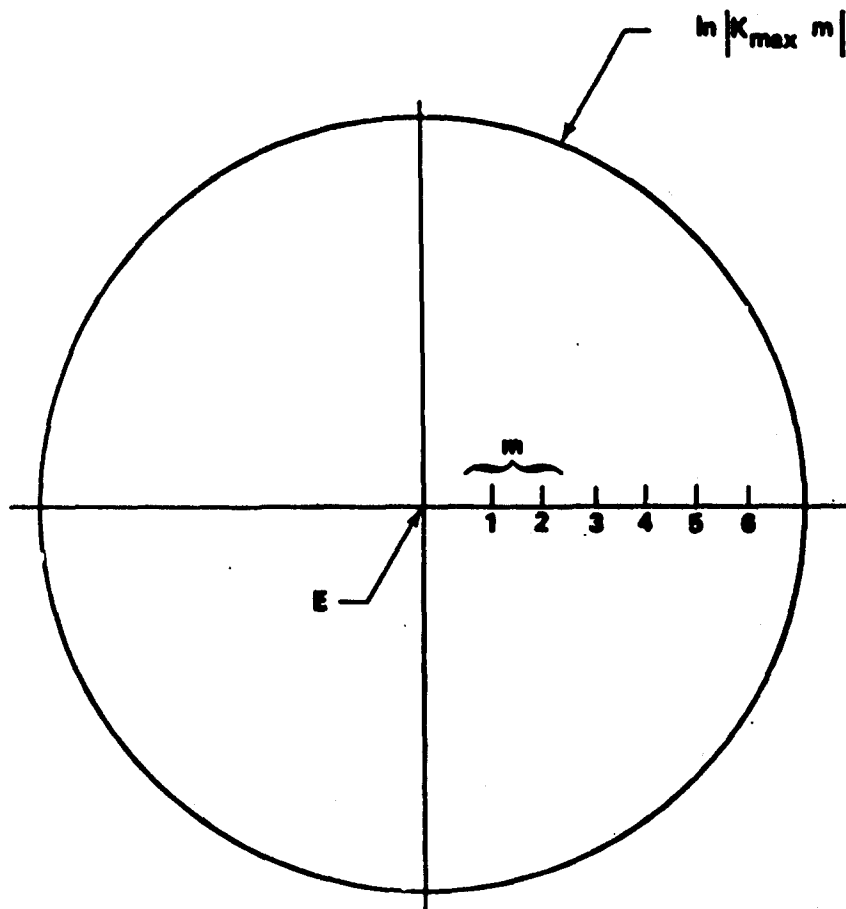


Figure 4. Equipotentials at discrete intervals.

Therefore excluding all other considerations, a circular sheet of any size with applied potentials as defined represent a perfect device in reflecting Equation (12). Other considerations limit the size to some minimum and these considerations will be discussed.

The ICING Research Staff [5] investigated a number of possible conductive materials and their findings can be summarized as follows to eliminate a number of approaches:

1. Metal foils are too low in resistivity.
2. Metallic coated conductors have unacceptable variations in space conductivity.
3. Electrolytic conductors are best applied in tanks and therefore not suitable to the problem.
4. Teledeltos paper has disadvantages (previously discussed).
5. Conductive paint has some promise but production problems are rather strenuous.

One of the most potent designs available at present is the ESTAC computer [7]. This device uses the Factor Analog method with a large carbon conductor sheet. It requires setting and manipulation of pole-zero probes and with the readout is approximately the size of a large desk. While it is an extremely useful device, it remains larger and more complex than the one being investigated.

One of the problems which becomes obvious is distortion of the field resulting from contacts with conductivity different from the film. The contacts themselves must be negligible relative to the overall area of the sheet. Measuring instrumentation input impedance must be kept large to prevent distortion. Coincident with these problems, the contact and measuring system must avoid the errors of unpredictable large contact drop.

In a relatively large sheet system where a movable small number of contacts are utilized, the problem is not as great as one with fixed

If d in Equation (12) is allowed to equal Km , where m = increment of distance measurement and K = number of increments internal, and if the potential is applied at a perfect circular contact on a limited sheet at the maximum k , all internal points are a perfect representation of Equation (12). This is shown in Figure 4.

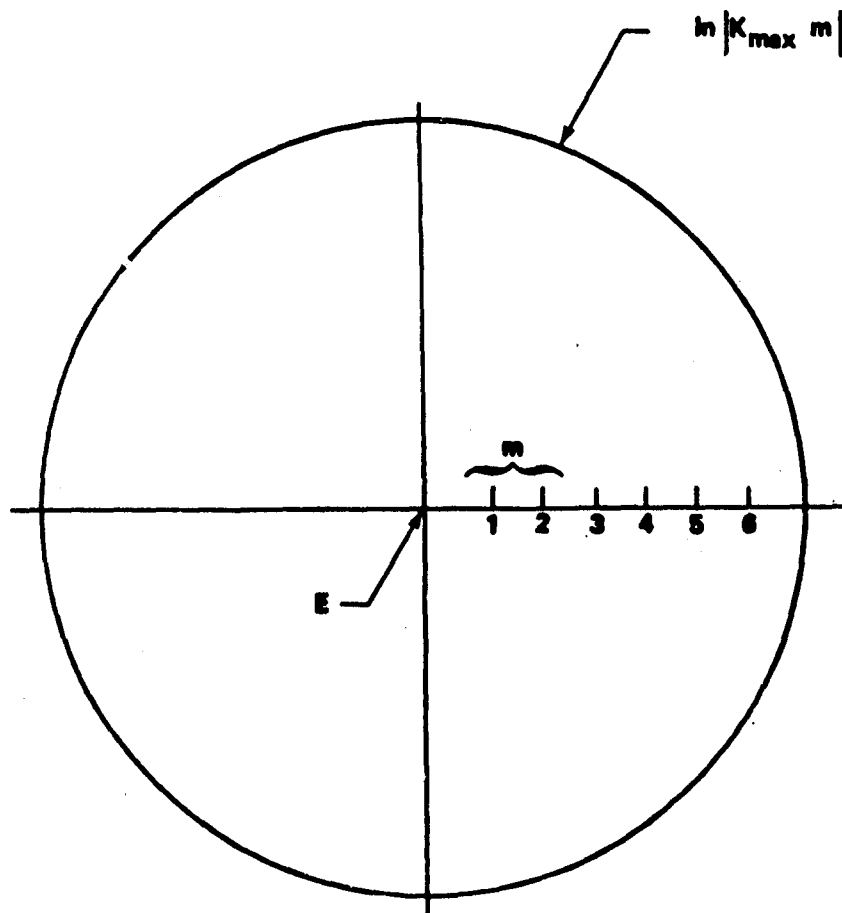


Figure 4. Equipotentials at discrete intervals.

Therefore excluding all other considerations, a circular sheet of any size with applied potentials as defined represent a perfect device in reflecting Equation (12). Other considerations limit the size to some minimum and these considerations will be discussed.

The ICING Research Staff [5] investigated a number of possible conductive materials and their findings can be summarized as follows to eliminate a number of approaches:

1. Metal foils are too low in resistivity.
2. Metallic coated conductors have unacceptable variations in space conductivity.
3. Electrolytic conductors are best applied in tanks and therefore not suitable to the problem.
4. Teledeltos paper has disadvantages (previously discussed).
5. Conductive paint has some promise but production problems are rather strenuous.

One of the most potent designs available at present is the ESIAC computer [7]. This device uses the Factor Analog method with a large carbon conductor sheet. It requires setting and manipulation of pole-zero probes and with the readout is approximately the size of a large desk. While it is an extremely useful device, it remains larger and more complex than the one being investigated.

One of the problems which becomes obvious is distortion of the field resulting from contacts with conductivity different from the film. The contacts themselves must be negligible relative to the overall area of the sheet. Measuring instrumentation input impedance must be kept large to prevent distortion. Coincident with these problems, the contact and measuring system must avoid the errors of unpredictable large contact drop.

In a relatively large sheet system where a movable small number of contacts are utilized, the problem is not as great as one with fixed

If d in Equation (12) is allowed to equal Km , where m = increment of distance measurement and K = number of increments internal, and if the potential is applied at a perfect circular contact on a limited sheet at the maximum k , all internal points are a perfect representation of Equation (12). This is shown in Figure 4.

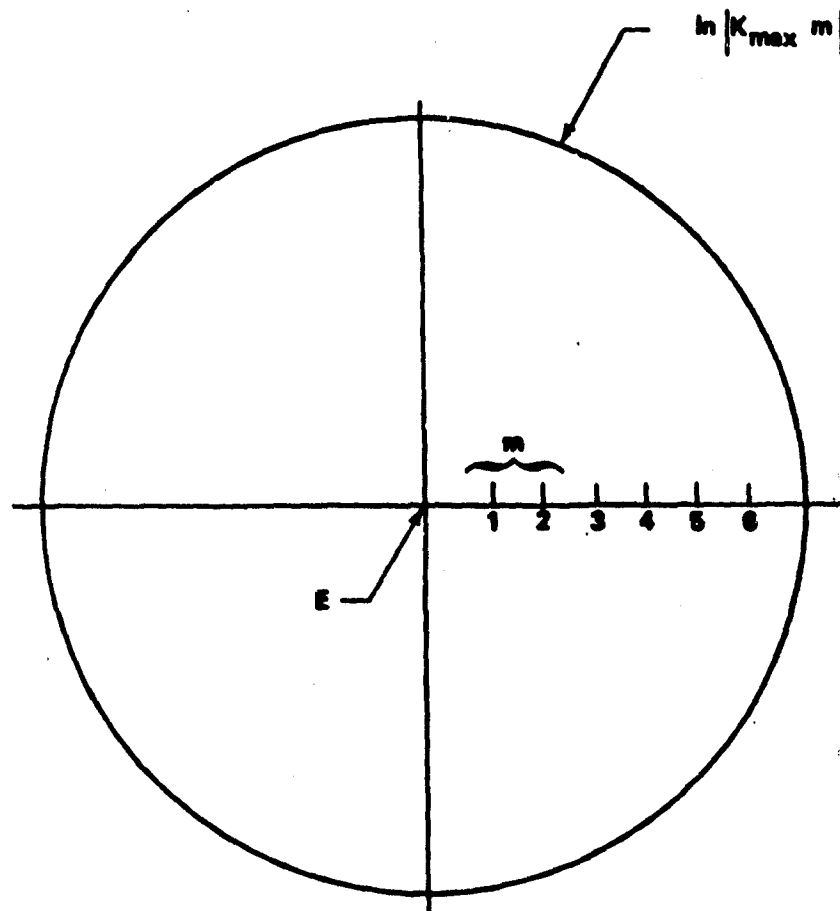


Figure 4. Equipotentials at discrete intervals.

Therefore excluding all other considerations, a circular sheet of any size with applied potentials as defined represent a perfect device in reflecting Equation (12). Other considerations limit the size to some minimum and these considerations will be discussed.

The ICING Research Staff [5] investigated a number of possible conductive materials and their findings can be summarized as follows to eliminate a number of approaches:

1. Metal foils are too low in resistivity.
2. Metallic coated conductors have unacceptable variations in space conductivity.
3. Electrolytic conductors are best applied in tanks and therefore not suitable to the problem.
4. Teledeltos paper has disadvantages (previously discussed).
5. Conductive paint has some promise but production problems are rather strenuous.

One of the most potent designs available at present is the ESIAC computer [7]. This device uses the Factor Analog method with a large carbon conductor sheet. It requires setting and manipulation of pole-zero probes and with the readout is approximately the size of a large desk. While it is an extremely useful device, it remains larger and more complex than the one being investigated.

One of the problems which becomes obvious is distortion of the field resulting from contacts with conductivity different from the film. The contacts themselves must be negligible relative to the overall area of the sheet. Measuring instrumentation input impedance must be kept large to prevent distortion. Coincident with these problems, the contact and measuring system must avoid the errors of nonpredictable large contact drop.

In a relatively large sheet system where a movable small number of contacts are utilized, the problem is not as great as one with fixed

If d in Equation (12) is allowed to equal Km , where m = increment of distance measurement and K = number of increments internal, and if the potential is applied at a perfect circular contact on a limited sheet at the maximum k , all internal points are a perfect representation of Equation (12). This is shown in Figure 4.

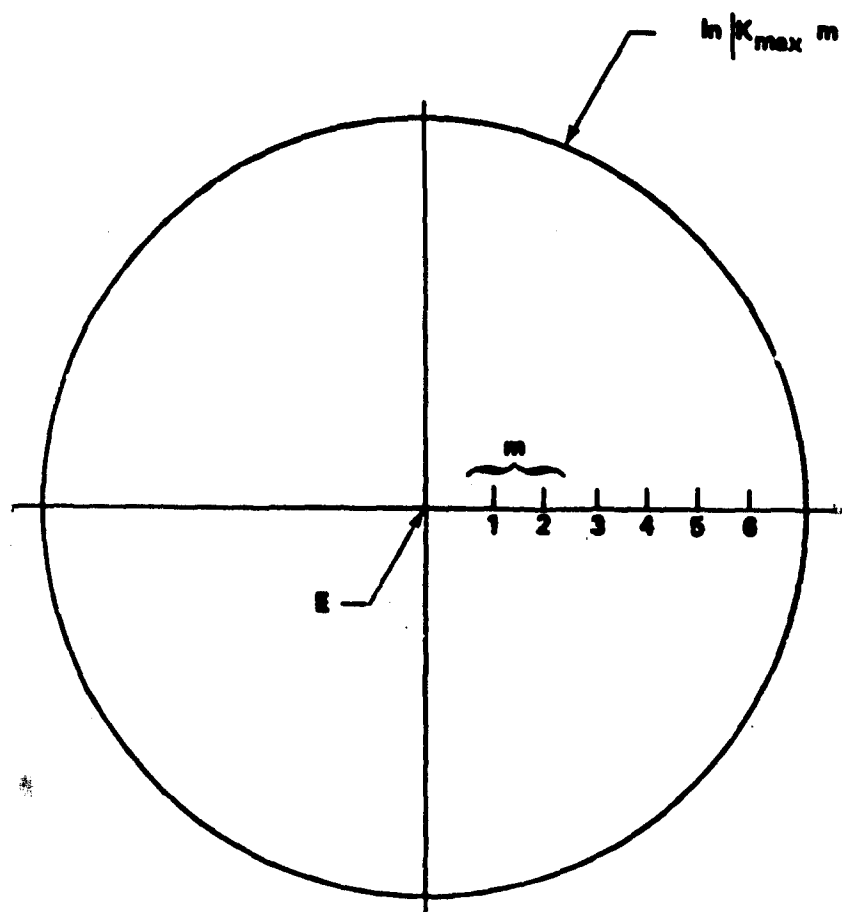


Figure 4. Equipotentials at discrete intervals.

Therefore excluding all other considerations, a circular sheet of any size with applied potentials as defined represent a perfect device in reflecting Equation (12). Other considerations limit the size to some minimum and these considerations will be discussed.

The ICING Research Staff [5] investigated a number of possible conductive materials and their findings can be summarized as follows to eliminate a number of approaches:

1. Metal foils are too low in resistivity.
2. Metallic coated conductors have unacceptable variations in space conductivity.
3. Electrolytic conductors are best applied in tanks and therefore not suitable to the problem.
4. Teledeltos paper has disadvantages (previously discussed).
5. Conductive paint has some promise but production problems are rather strenuous.

One of the most potent designs available at present is the ESIAC computer [7]. This device uses the Factor Analog method with a large carbon conductor sheet. It requires setting and manipulation of pole-zero probes and with the readout is approximately the size of a large desk. While it is an extremely useful device, it remains larger and more complex than the one being investigated.

One of the problems which becomes obvious is distortion of the field resulting from contacts with conductivity different from the film. The contacts themselves must be negligible relative to the overall area of the sheet. Measuring instrumentation input impedance must be kept large to prevent distortion. Coincident with these problems, the contact and measuring system must avoid the errors of nonpredictable large contact drop.

In a relatively large sheet system where a movable small number of contacts are utilized, the problem is not as great as one with fixed

contact. Where this fixed contact scheme is utilized, the number between the center source and outer ring is of importance because this controls the range of frequencies over which a function can be investigated on a single wafer.

The mechanical accuracy to which a measuring point can be deposited controls the accuracy which can be obtained.

This placement accuracy is of most importance when measurements are made near wafer center. This becomes obvious from Equation (12) if we let Δd equal the magnitude of uncertainty. A diagram of the wafer is shown in Figure 4 with necessary constants indicated. Then

$$\begin{aligned} |E_m| &= E \ln |d + \Delta d| \\ &= E \ln |d + 0.001 \text{ inch}| \end{aligned}$$

with a 0.03-inch displacement

$$\begin{aligned} (\text{Error}) &= E \ln |0.031| - E \ln |0.030| \\ &= E(0.0288) \end{aligned}$$

If measurement accuracy from an instrumentation aspect is considered, then the total (i.e., predictable drop such as instrument accuracy, distortion resulting from instrument drain, etc.) of all effects must be considered. These effects predominate at the extreme wafer edge where voltage differences are small relative to placement.

Instrument errors will in general follow as a fixed value (i.e., percent full scale) and hence will have significance when considering small voltages.

Then where electrical measurement accuracy only is considered

$$E_m = E_a + \Delta e$$

where we consider only one direction of error and

E_m = measured voltage

E_a = actual voltage

Δe = error in voltage.

If we consider that some percentage of accuracy is required, then at all times

$$\text{Percent error} = 2.88 + \left| \frac{\Delta e}{E_a} \right| 100$$

$\Delta e = 0.01$ volt is reasonable

$$\text{Percent error} = 2.88 + \frac{1}{E_a} .$$

Then for a four percent system

$$E_{\min} = 0.893 .$$

This indicates a worst case feasibility and therefore the final device should approximate three percent near center and nearer one percent at extremes of the wafer.

Most of the present general-use systems satisfy a requirement of ten percent accuracy. Because the device being considered is for even more general use than present units, it would appear that more than sufficient margin exists for attainable material characteristics.

CHAPTER IV

EXPERIMENTAL PROCEDURE AND RESULTS

I. RESISTANCE EXPERIMENTS

A number of familiarization experiments were conducted during the latter part of 1969 through the first part of 1970 using Teledeltos paper with a conductor painted circumference. Measurements of this type were used as a basis for a report by Huebschmann and Pender [2].

A number of silicon wafers were obtained and pick-off measurements were attempted. There was no success in this venture and the generation of the desired logarithmic function could not be obtained. While tungsten tip probes were used and data were obtained, it was too erratic for analysis. It was assumed that poor contacts or the diode effect was the prime causes for poor data, but experimental facilities were not available to verify these assumptions.

It was postulated that some basic measurements should be made on the material in an attempt to determine whether either or both effects existed and which was predominant.

Initial tests were made to determine the effects of instrument insertion and thereby allowed removal of these from consideration. The mechanical arrangement is shown in Figure 5. The voltmeter used, was a Fairchild model 259 and the Ammeter was a Data Technology model DT 360.

Data from this experiment are presented in Table 1 and include results of several repetitive tests made over the total range.

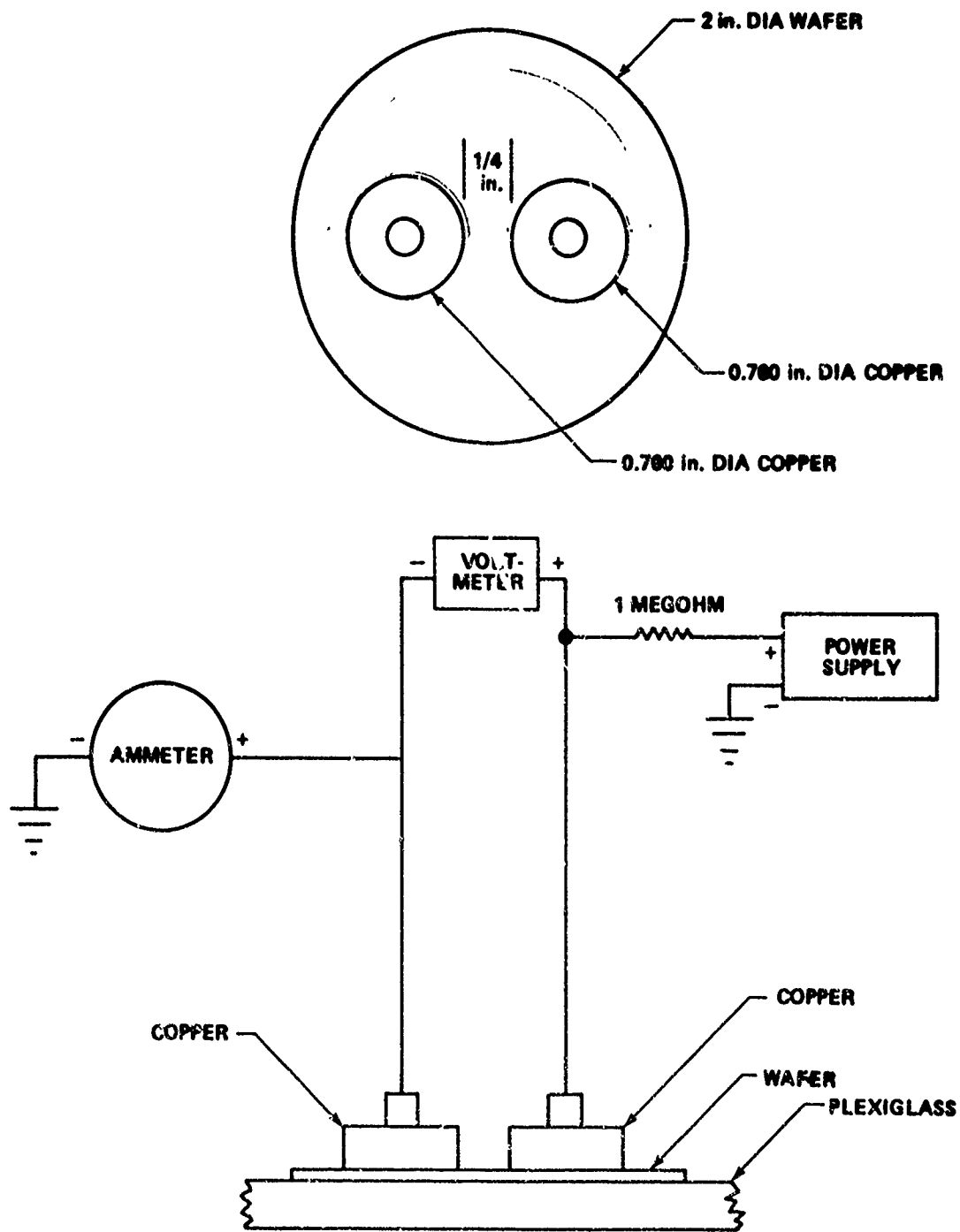


Figure 5. Longitude dimension resistance experiment.

Table I. Longitude dimension resistance, test 1

Volts	Current (Ma)	Resistance (Kohms)
5.32	0.03	177
8.35	0.05	167
15.4	0.10	154
29.2	0.20	146
69.3	0.50	138
130.9	1.00	130
206.0	1.99	103
285.0	3.14	91
399.0	3.50	114

This experiment indicated that at least some diode effect appeared and that resistance characteristics of the material were too high. It was reasoned that a further test with the mechanical arrangement as shown in Figure 6 would enhance any diode effect.

The data from this experiment are given in Table 2 with presentation in Figures 7 and 8. These data were verified by a number of tests over the total data span. The tunnel effect was observed at precisely 16.7 milliamperes on each test. At this point the voltage across the wafer began to drop and the current increased to the limits of the power supply. Because of facility limits, this phenomenon was pursued no further.

The curve from these data clearly indicated the diode effect and gave direction to part II of the experimental process. It also became evident that lower resistive materials and better contacts were necessary.

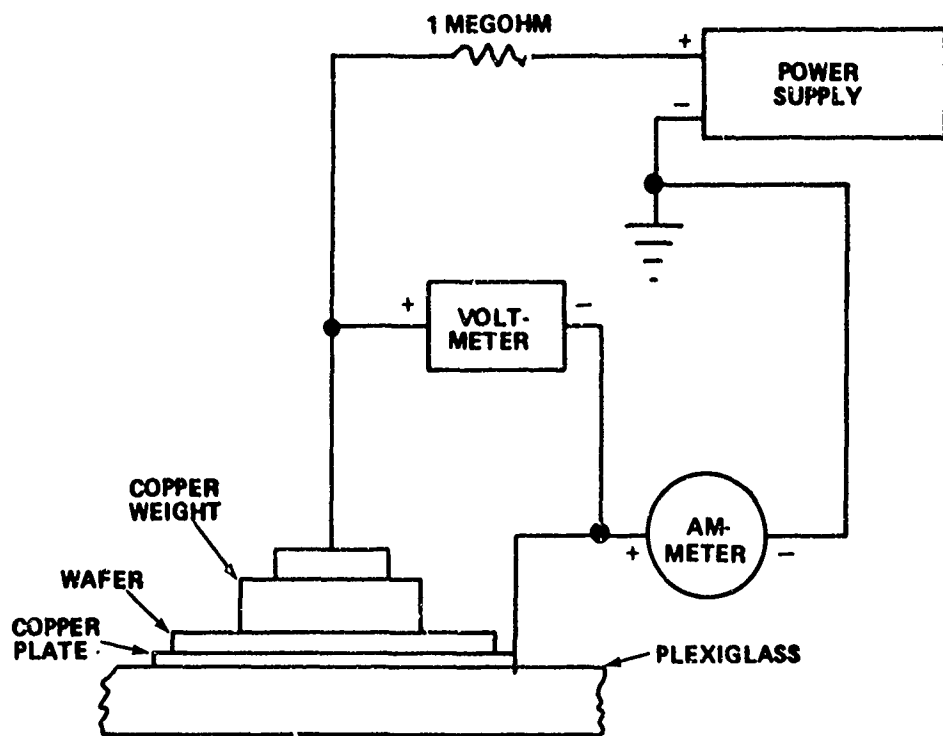
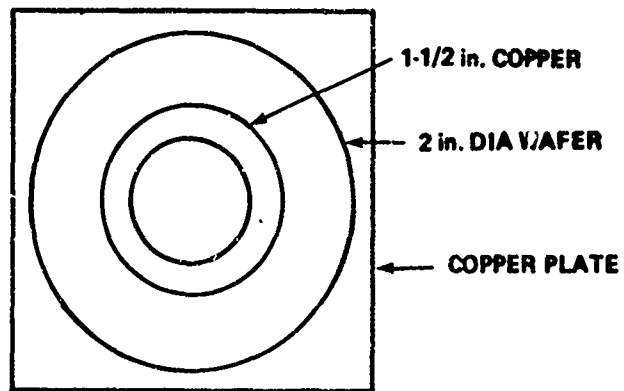


Figure 6. Thin dimension resistance experiment.

Table 2. Thin dimension resistance, test 2

Volts	Current (Ma)	Resistance (Kohms)
5.6	0.03	186
7.5	0.05	150
11.5	0.10	115
17.1	0.20	85
29.7	0.50	59
43.3	1.00	43
66.1	2.02	33
82.8	3.00	28
97.6	4.04	24
109.0	5.18	21
124.7	7.02	18
143.8	10.10	14
155.1	14.00	11
160.6	16.70	10

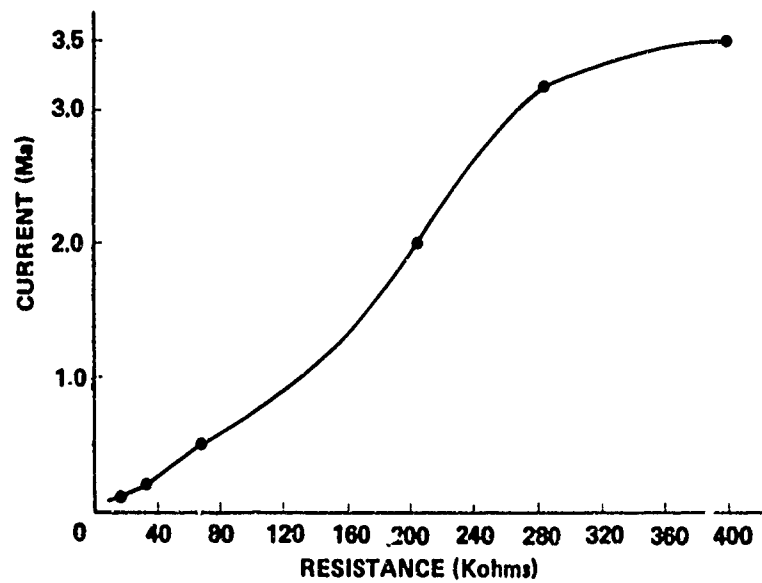


Figure 7. Graph of the thin dimension resistance.

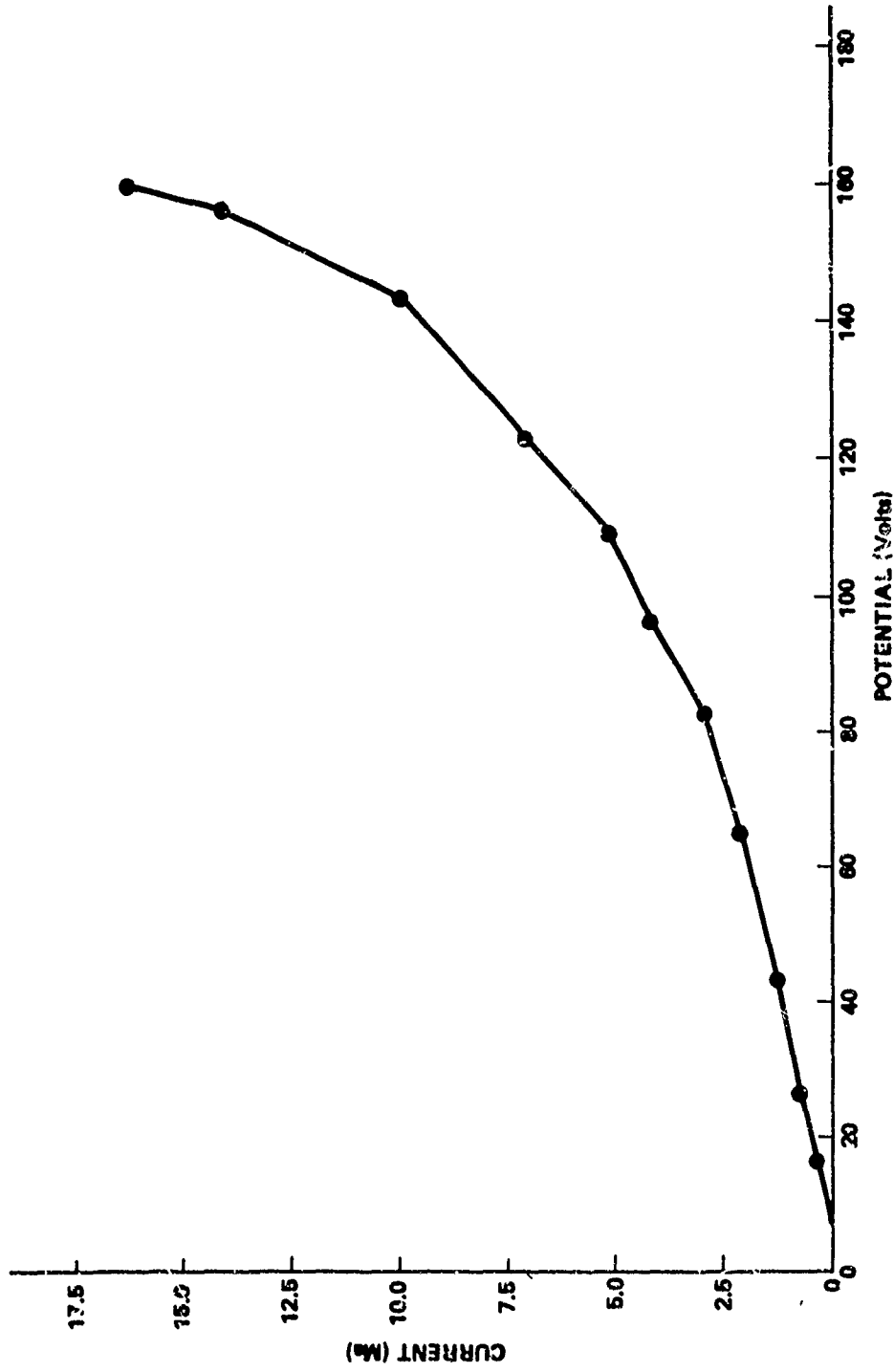


Figure 8. Diode effect in thin dimension experiment.

II. LINEARITY EXPERIMENTS

At this point in experimentation, two wafers were constructed by Astrionics Laboratory of Marshall Space Flight Center. Wafer processing information has been furnished (with proprietary limitations) by this laboratory.

Processing Information:

1. Wafer specifications:

Resistivity 3-5 ohms/centimeter; N type, phosphorous doped

Orientation: 111

Wafer thickness: 7-10 mils

2. Standard clean:

85°C H₂SO₄: HNO₃ (2:1) 10 minutes

Deionized and distilled (DI) H₂O rinse for 10 minutes

Ultrasonic trichloroethylene (TCE) rinse - 10 minutes

Ultrasonic acetone (ACE) rinse - 10 minutes

DI H₂O rinse for 10 minutes

Blow dry with N₂

3. Diffusion: 980°C furnace

Dopant - Boron

Source - Diborane

Time - 60 minutes

Ohms/centimeter after predip = 27

4. Oxidation: 1150°C

Steam with O₂ carrier for 40 minutes

5. Strip oxide with buffer HCl etch
Ohms/square = 180-200
6. Premetal clean
DI H₂O rinse - 10 minutes
ACE ultrasonic rinse - 10 minutes
DI H₂O rinse - 10 minutes
Blow dry with N₂
7. Metallization
Evaporate aluminum at 10⁻⁶ more of Hg using electron
beam gun. Aluminum thickness = 8KÅ
8. Coat wafers with Kodak thin film photoresist
9. Align metallization mask and expose
10. Etch away unwanted aluminum
11. Alloy aluminum
555°C furnace for 5 minutes in N₂ ambient
12. Ready to test.

Measurements were made at the Astrionics Laboratory. Photographs of laboratory equipment are shown in Figures 9 through 12. Because of the physical (size) limitations on the probe station, it was necessary to rotate the test sample for various axial readings. In the process of doing this, the first sample was shattered.

In the process of taking measurements on the second sample, probe movement etched off the center wafer contact before final data on the fourth axis could be completed. An expanded photograph of this wafer is shown in Figure 13. The connections for measurement in circuit diagram form are shown in Figure 14.

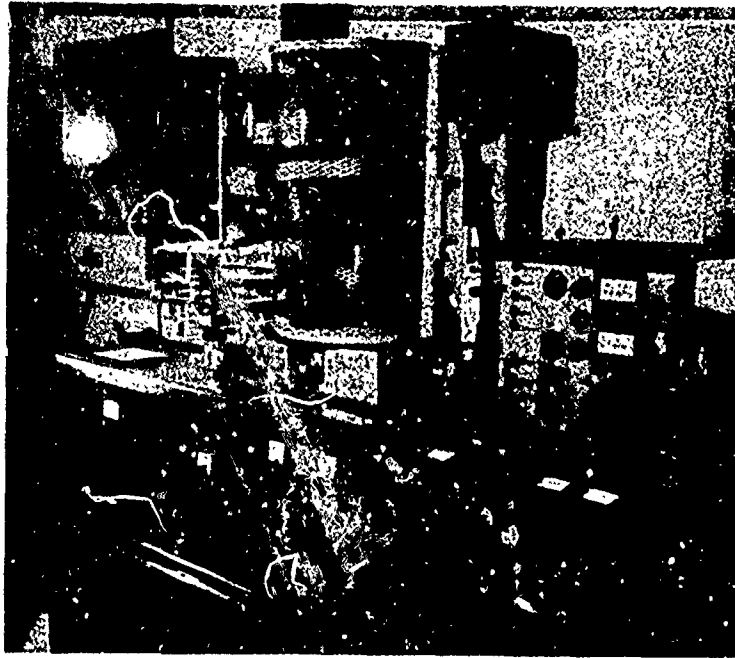


Figure 9. Vacuum chamber.



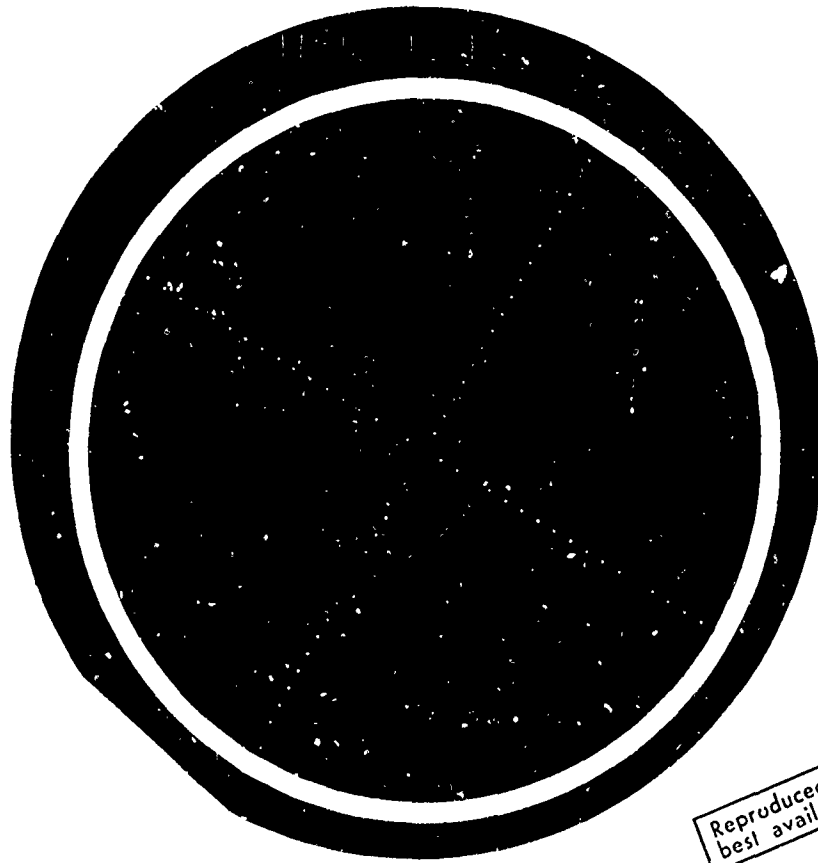
Figure 10. Testing circuits.



Figure 11. Placing wafers in furnace.



Figure 12. Photolithography room.



Reproduced from
best available copy.

Figure 13. Wafer 2 used in linearity experiments.

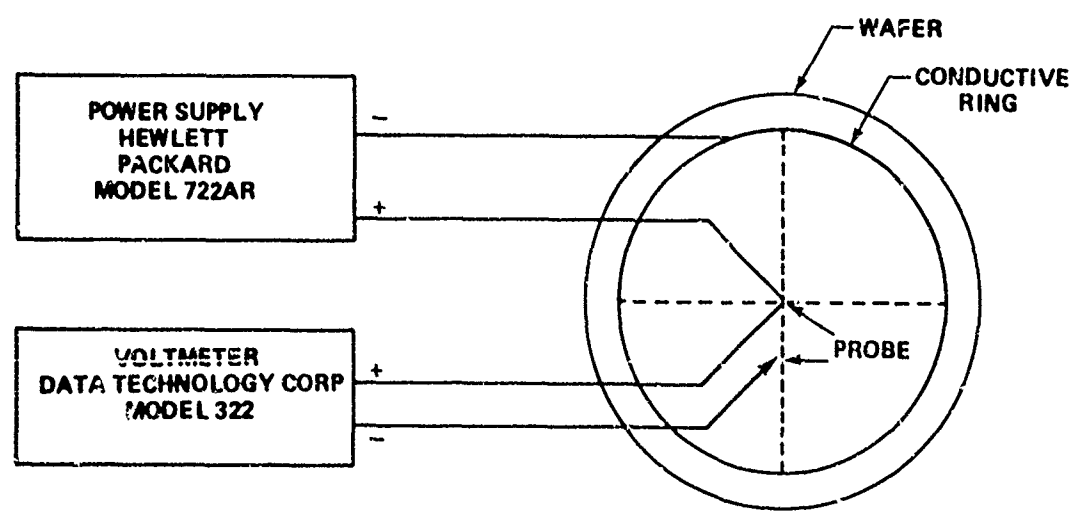


Figure 14. Measurement procedure utilized in linearity experiments.

The initial experimental data are shown in Table 3. Because of limits on the probe station (three probes), the outside conductor drop became a factor. A correction factor was required and applied ($E_c = E_{in} - E_{ring}$) with the final tabular results being listed in Table 4. A column has also been used to generate the average in this table and a plot around this average is shown in Figure 15. The last column in Table 4 indicates the worst percentage variation by point relative to the average. These numbers indicate that the tolerance is well within the desired range from a material standpoint.

The curve plotted in Figure 15 is a distorted representation of the infinite plane because the outer ring was held at an arbitrary potential. This can be corrected for by calculation if there is no distortion other than the ring potential problem at the outer edge. The correction involves one of assuming that the first measurement point from center is correct, calculating an outer ring potential, and correcting each internal point from this.

If points 1 and 2 are satisfactory then:

$$K_1 \ln m = 4.797$$

$$K_1 \ln 2m = 5.933$$

$$K_1 = 4.797/\ln m$$

$$\ln 2m = \ln 2 + \ln m$$

$$\ln m = 2.927$$

$$K_1 = 1.639$$

Table 3. Linearity experiments, wafer 1

Point	Radius 1	Radius 2	Radius 3	Radius 4	Comments
1	4.365	4.731	4.346	4.553	
2	5.498	5.792	5.559	5.831	
3	6.192	6.563	6.227	6.568	
4	6.863	6.976	6.798	7.246	
5	7.669	7.215	7.184	7.891	Radius 1
6	7.621	7.521	7.544	7.837	Questionable
7	7.755	7.997	7.750		
8	7.996	8.059	8.000		
9	8.183	8.295	8.448		
10	8.321	8.470	8.597		
11	8.522	8.652	8.660		
12	8.662	8.742	8.909		
13	8.820	8.897	9.019		
14	8.959	9.028	9.156		
15	9.142	9.103	9.312		
16	9.265	9.222	9.464		
17	9.434	9.575	9.493		
Ring	9.698	9.716	9.613		
Correction	0.294	0.276	0.379		$E_i = 9.992$

Table 4. Ring corrected results, wafer 1

Point	Radius 1	Radius 2	Radius 3	Average	Variance (percent)
1	4.659	5.007	4.725	4.797	4.4
2	5.792	6.068	5.938	5.933	2.4
3	6.486	6.839	6.606	6.644	2.9
4	7.157	7.252	7.177	7.193	0.8
5	7.963*	7.491	7.563	7.527	0.5
6	7.915	7.797	7.923	7.878	1.0
7	8.049	8.273	8.129	8.150	1.5
8	8.290	8.335	8.379	8.335	0.5
9	8.477	8.571	8.827	8.625	2.3
10	8.615	8.746	8.976	8.779	2.2
11	8.816	8.928	9.039	8.938	1.2
12	8.956	9.108	9.288	9.087	2.2
13	9.114	9.173	9.398	9.228	1.8
14	9.253	9.304	9.535	9.364	1.8
15	9.436	9.379	9.691	9.502	2.0
16	9.559	9.498	9.843	9.633	2.2
17	9.728	9.851	9.872	9.817	0.9
Ring	9.992	9.992	9.992	9.992	

*Take out in average.

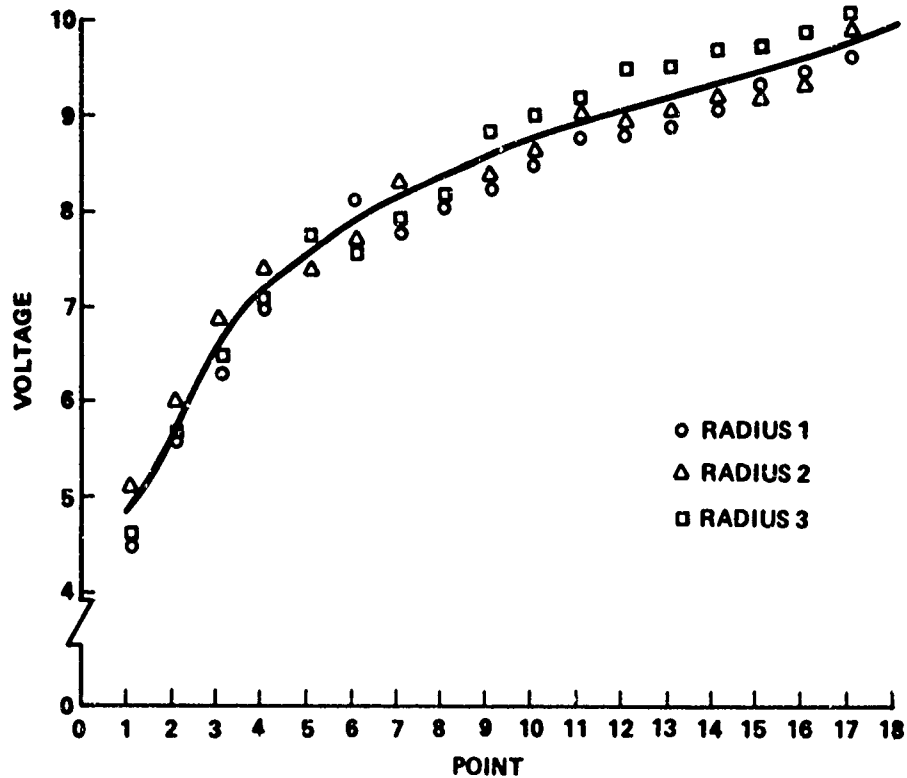


Figure 15. Graph of linearity experiment results.

Data calculated on this basis are shown in column 3 of Table 5. Using the same type of calculation, column 4 indicates the first and last data fit. Column 3 was calculated on data points 3 and 6 and reveals a much closer fit with measured data.

Column 3 clearly indicates the center contact distortion while column 4 illustrates the conductive ring problem. The last point distortion was surmised to be an error in distance between it and the outer ring. Examination under a microscope proved this to be true.

This phase of experimentation indicated that the material could be held to sufficient isotropic characteristics for the application.

Table 5. Theoretical curve fit, wafer 1

Point	Measurement	Calculation 1 and 2	Calculation 1 and 17	Calculation 3 and 6
1	4.797	4.797	4.797	4.88
2	4.933	4.933	6.025	5.922
3	6.644	6.598	6.743	6.644
4	7.193	7.0695	7.253	7.156
5	7.527	7.4352	7.648	7.553
6	7.878	7.734	7.792	7.878
7	8.150	7.9866	8.245	8.152
8	8.335	8.2055	8.481	8.390
9	8.625	8.3986	8.690	8.600
10	8.779	8.5713	8.877	8.787
11	8.928	8.7275	9.046	8.937
12	9.087	8.8701	9.200	9.111
13	9.228	9.0012	9.342	9.254
14	9.364	9.1228	9.493	9.384
15	9.502	9.2358	9.595	9.509
16	9.633	9.3416	9.709	9.624
17	9.817	9.4410	9.817	9.732
Ring	9.992			

These findings are valid despite the distortion. A further experiment on wafers of this form was planned to verify these results and to further separate problems.

At the same time wafers with one-fourth the number of measurement points along each axis were requested in an attempt to remove the linear distortion. An increase in conductor ring width was made to alleviate the problem caused by ring conductor drop.

III. CONTACT AND FUNCTION EXPERIMENTS

Contact and function experiments were initiated with a number of inherent problems. These problems and the action taken to alleviate them are presented in the following paragraphs.

Considerable distortion was experienced beyond even the second point which apparently resulted from the heating effect. This was countered to some extent by lowering the voltage from 10 to approximately 6 volts therefore reducing power by almost two-thirds.

Ring drop (resulting from current in the conductor) was causing a distortion which could not reasonably be accounted for. Two additional probes were assembled and located around the conducting ring. Observation of resulting data indicated that this maintained the conducting ring, within measurement tolerance, at equipotential around the circumference.

The center-located (current insertion) probe destroyed the aluminum deposit because of a constant necessity for manipulation. The probe used was filed to round the point. The same problem was encountered in sample one of this phase but further work on the probe

alleviated this problem on sample two. It did, however, develop as a source of erratic contact which shall be discussed in the data analysis of this phase.

The problem of wafer contact size and field distortion could not be dealt with because of equipment resources. A method of countering this problem will be discussed in the conclusions and recommendations of this report.

Data taken on wafer 1 are tabulated in Table 6. The maximum percent error around the average is 5.5 percent which is within tolerance for this effort.

Table 7 has three columns with the first representing average data from Table 6. The second column represents computed values using points one and two as coincident with an idealized curve. The third column indicates percentage difference. The distortion problem around the center appeared under control with the lower voltage.

Tables 8 and 9 show the corresponding values for wafer 2 and agree reasonably with the wafer 1 test. To evaluate the probe manipulation, problem data were recorded. Figure 16 is a plot of these data and indicates an error bias resulting from this effect.

In an attempt to determine the status of producing a Laplace function with accuracy and prior to part IV, the program shown in Table 10 was constructed. The reasoning for this program is based upon the following equations.

If we wish to represent two decades on the wafer (i.e., 1-10, 10-100) then with 17 contacts:

$$K_D = \frac{17}{100} = 0.17 \text{ contact separation per frequency unit.}$$

Table 6. Contact and function results, wafer 1

Point	Radius 1	Radius 2	Radius 3	Radius 4	Average	Maximum Error Around Average (percent)
Center	6.002	6.002	6.002	6.004		
1	2.383	2.436	2.427	2.420	2.416	-1.4
2	1.810	1.882	1.867	1.847	1.852	-2.27
3	1.536	1.533	1.549	1.540	1.540	+0.58
4	1.285	1.333	1.301	1.311	1.308	+1.91
5	1.125	1.118	1.148	1.136	1.132	+1.41
6	0.975	0.935	0.958	0.954	0.956	+2.5
7	0.870	0.896		0.904	0.890	-2.2
8	0.736	0.739		0.747	0.740	+0.95
9	0.647	0.652		0.662	0.654	+1.22
10	0.576	0.559		0.556	0.564	±2.13
11	0.505	0.487		0.506	0.499	-2.4
12	0.427	0.398		0.409	0.411	+3.9
13	0.376	0.342		0.359	0.359	+4.7
14	0.311	0.289		0.319	0.306	-5.5
15	0.250	0.237		0.245	0.244	-2.9
16	0.207	0.206		0.215	0.219	+2.9
17	0.175	0.165		0.160	0.167	+4.8
Ring	0.047	0.055	0.050	0.050		

Table 7. Theoretical curve fit, wafer 1

Point	Measurement	Points 1 and 2	Error (percent)
1	3.586	3.586	0
2	4.150	4.150	0
3	4.462	4.480	0.4
4	4.694	4.714	0.4
5	4.870	4.896	0.5
6	5.046	5.044	0.04
7	5.112	5.169	1.10
8	5.262	5.278	0.3
9	5.348	5.374	0.5
10	5.438	5.460	0.4
11	5.503	5.537	0.6
12	5.591	5.608	0.3
13	5.643	5.673	0.5
14	5.696	5.734	0.6
15	5.758	5.790	0.6
16	5.793	5.842	0.8
17	5.825	5.891	0.9
Ring	5.952		

Table 8. Contact and function results, wafer 2

Point	Radius 1	Radius 2	Radius 3	Radius 4	Average	Maximum Error Around Average (percent)
Center	6.342	6.342	6.342	6.342		
1	3.216	3.262	3.248	3.129	3.216	-2.4
2	2.417	2.420	2.416	2.437	2.448	+2.8
3	2.078	2.086*	2.087	2.018*	2.067	-2.4
4	1.726	1.720	1.715	1.654	1.704	-0.73
5	1.417	1.470	1.461	1.469	1.454	-2.5
6	1.306	1.276	1.297	1.318*	1.274	-4.4
7	1.099	1.085	1.146*	1.063*	1.099	+4.3
8	0.935	0.955	0.977	0.967	0.959	-2.5
9	0.793	0.835	0.841	0.784*	0.813	-3.6
10	0.661	0.715	0.702	0.670	0.687	+4.1
11	0.583	0.633*	0.604	0.581*	0.600	+5.5
12	0.476	0.514	0.501*	0.489	0.495	±3.8
13	0.375	0.400	0.395*	0.369*	0.384	-4.16
14	0.285	0.294	0.305*	0.275*	0.289	+5.5
15	0.225	0.240	0.242	0.227	0.234	-3.9
16	0.151	0.163	0.160	0.153	0.156	+4.5
17	0.084	0.085	0.083	0.079*	0.083	-4.8
Ring	0.040	0.041	0.040	0.040		

*Probe adjustment at these measurements.

Table 9. Theoretical curve fit, wafer 2

Point	Measurement	Points 1 and 2	Error (percent)
1	3.126	3.126	0
2	3.894	3.894	0
3	4.275	4.342	1.5
4	4.638	4.662	0.5
5	4.888	4.909	0.4
6	5.068	5.111	0.8
7	5.243	5.282	0.7
8	5.383	5.430	0.8
9	5.529	5.560	0.5
10	5.655	5.677	0.4
11	5.742	5.783	0.7
12	5.847	5.879	0.5
13	5.958	5.968	0.2
14	6.053	6.050	0.05
15	6.108	6.126	0.3
16	6.186	6.198	0.2
17	6.259	6.265	0.1
Ring			

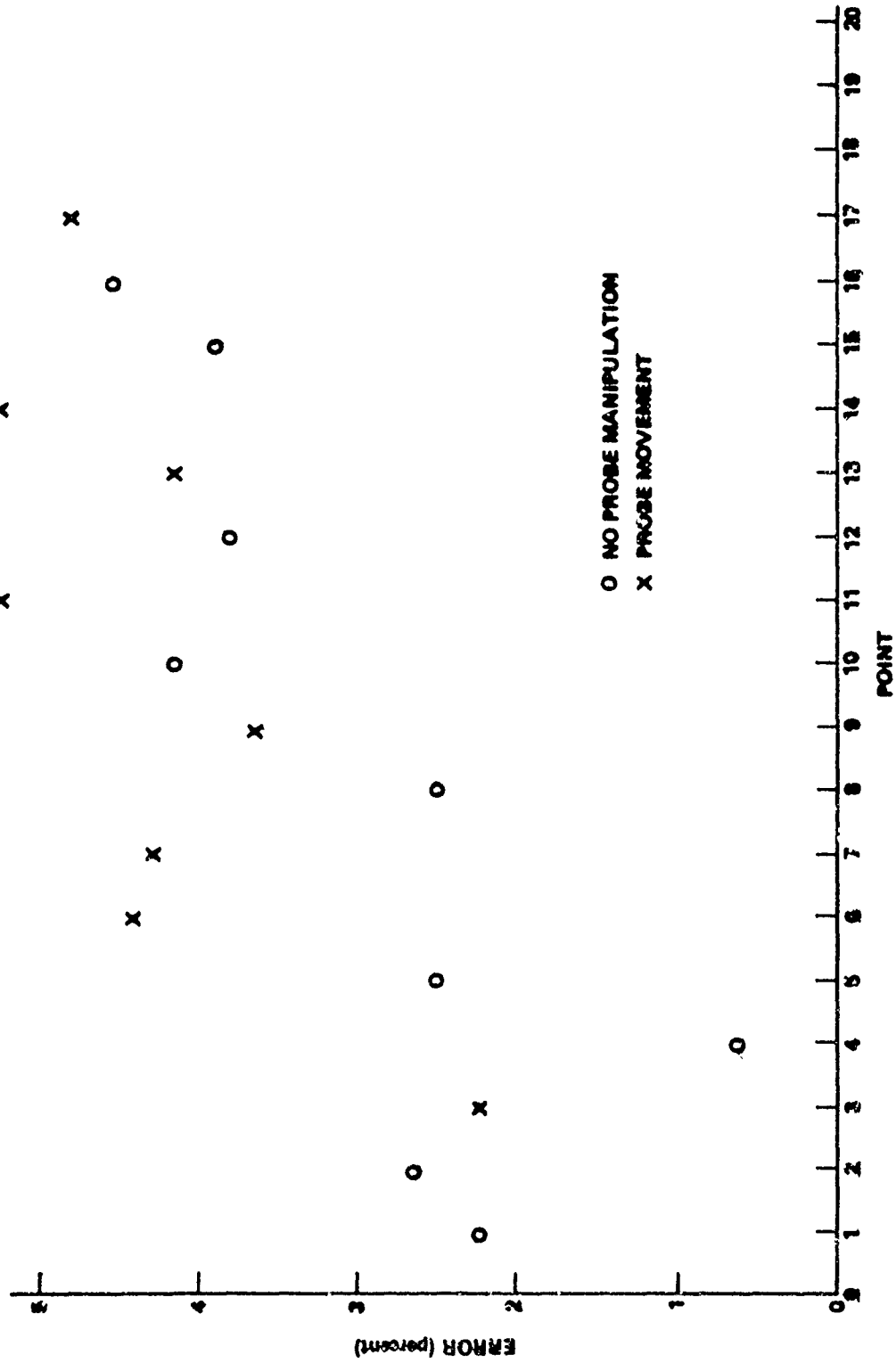


Figure 16. Probe fixture manipulation and error effect.

Table 10. Program listing function generation

```

TRANSF
C
C EVALUATION OF BROWN TRANSFER FUNCTION NO. 2
C TRAN. FUNC.  $=(S-10+J3)(S-4+J6)/(S+3+J7)(S-6+J10)$ 
C COMPLEX FU(4),FC(4),S,TFC0,TFC1,TFC13,TFC40
C REAL FMAG(4),FLOG(4),PTRSF,FREQ,EXPMF(4),CK2(4),CK3(4),VEXP(17)
C READ 2,FU
C 2 FORMAT(8F6,1)
C DO 4 I=1,17
C READ 3, EPOS
C 3 FORMAT(5X,F10.3)
C 4 VEXP(I)*EPOS
C CK1=1.108
C S=(0.0,-20.0)
C FIND VALUES OF CONSTANTS
C DO 9 N=1,4
C TFC0=FU(N)
C TFC1=(0.0,1.0)+FU(N)
C TFC13=(0.0,13.0)+FU(N)
C TFC40=(0.0,40.0)+FU(N)
C TFM0=CABS(TFC0)
C TFM1=CABS(TFC1)
C TFM13=CABS(TFC13)
C TFM40=CABS(TFC40)
C TFLN0=ALOG(TFM0)
C TFLN1=ALOG(TFM1)
C TFLN13=ALOG(TFM13)
C TFLN40=ALOG(TFM40)
C TDEL0=0.17*TFM0
C TDEL1=0.17*TFM1
C TDEL13=0.17*TFM13
C TDEL40=0.17*TFM40
C IDIS0=INT(TDEL0)
C IDIS1=INT(TDEL1)
C IDIS13=INT(TDEL13)
C IDIS40=INT(TDEL40)
C REM0=TDEL0/FLOAT(IDIS0)
C REM1=TDEL1/FLOAT(IDIS1)
C REM13=TDEL13/FLOAT(IDIS13)
C REM40=TDEL40/FLOAT(IDIS40)
C VAL0=VEXP(IDIS0)+CK1*ALOG(REM0)
C VAL1=VEXP(IDIS1)+CK1*ALOG(REM1)
C VAL13=VEXP(IDIS13)+CK1*ALOG(REM13)
C VAL40=VEXP(IDIS40)+CK1*ALOG(REM40)
C CK2(N)=(TFLN1-TFLN0)/(VAL1-VAL0)
C TEMPA=TFLN40-(VAL40-VEXP(1))*CK2(N)
C TEMPB=TFLN13-(VAL13-VEXP(1))*CK2(N)
C CK3(N)=(TEMPA+TEMPB)/2.0
C PRINT 999,CK2(N),CK3(N)
999 FORMAT(20X,2F10.4)
9 CONTINUE
PRINT 5
5 FORMAT(1H1,2X113HFREQ MF1(S) EXPF1(S) MF2(S) EXPF2(S)
XMF3(S) EXPF3(S) MF4(S) EXPF4(S) CAL.TRS EXP.TRS ERROR/)
C EVALUATE COMPLEX FUNCTION,MODULUS,AND NATURAL LOG.
C DO 20 I=1,49
C DO 17 J=1,4
C FC(J)=S+FU(J)
C FMAG(J)=CABS(FC(J))

```

Table 10. (continued)

```

TRANSF
FLOG(J)=ALOG(FMAG(J))
DFLR=0.17*FMAG(J)
IDIST=INT(DELR)
IF(IDIST.EQ.0) IDIST=1
REMX=DELR/FLOAT(IDIST)
VAL2=VEXP(IDIST)+CK1*ALOG(1EMX)
EXPMF(J)=CK2(J)*(VAL2-VEXP(1))+CK3(J)
17 CONTINUE
C EVALUATE TRANSFER FUNCTION
FTRSF=FLOG(1)+FLOG(2)-FLOG(3)-FLOG(4)
EXPTR=EXPMF(1)+EXPMF(2)-EXPMF(3)-EXPMF(4)
VTRSF=EXP(FTRSF)
VXPTR=EXP(EXPTR)
ERROR=((VTRSF-VXPTR)/VTRSF)*100.0
FREQ=AIMAG(S)
PRINT 99,FREQ,( FLOG(K),EXPMF(K) ,K=1,4),VTRSF,VXPTR,ERROR
99 FORMAT(2X,F6.1,10F10.4,F9.1)
IF(I.GE.41) GO TO 19
S=S+(0.0,1.0)
GO TO 20
19 S=S+(0.0,10.0)
20 CONTINUE
STOP
END
0000 ERRORS. COMPILATION COMPLETE.

.9025 1.7915
.9025 1.7815
.9025 1.7815
.9025 1.7815

```

Further using the first two data points on wafer 2,

$$K_1 \ln m = 3.126$$

$$K_1 \ln 2m = 3.894$$

$$K_1 = 1.108$$

$$\ln m = 2.8213$$

which will allow voltage interpolation between points.

Four functions in the form

$$F(S) = \frac{(S + 10 - j3)(S + 4 - j6)}{(S - 3 - j7)(S + 6 - j10)}$$

were selected and are listed in Table 11 as follows:

$$F_1(s) = S + 10 - j3$$

$$F_2(s) = S + 4 - j6$$

$$F_3(s) = S - 3 - j7$$

$$F_4(s) = S + 6 - j10$$

The natural logarithm of each function is listed as a function of frequencies. In the program, scale factors are first calculated as

$$\ln|F(s_1)| - \ln|F(s_1)| = K_2(\text{EXP } 1 - \text{EXP } 2)$$

and a reference reading as

$$K_3 = \frac{\text{EXP } 40 - \ln|F(s_{40})| + \text{EXP } 13 - \ln|F(s_{13})|}{2}$$

and

$$\text{EXP } 40 = \ln K_d |F(s_{40})|^m$$

This results in a form of a whole number and some number of decimal places such as:

$$\begin{aligned} &= \ln (A.BCDEF) m \\ &= \ln A_m + \ln \frac{A.BCDEF}{A} \end{aligned}$$

where A_m represents the reading at a particular point and the second term is an interpolation factor.

Table 11. Computer function generation

FREQ	MF1(S)	EXPF1(S)	MF2(S)	EXPF2(S)	MF3(S)	EXPF3(S)	MF4(S)	EXPF4(S)
-20.0	3.2221	3.2199	3.2698	3.2577	3.3020	3.2899	3.4208	3.4112
-19.0	3.1850	3.1828	3.2315	3.2194	3.2647	3.2526	3.3883	3.3787
-18.0	3.1467	3.1046	3.1918	3.1797	3.2260	3.2139	3.3547	3.3426
-17.0	3.1073	3.0652	3.1504	3.0984	3.1858	3.1737	3.3199	3.3079
-16.0	3.0667	3.0246	3.1073	3.0553	3.1439	3.0919	3.2840	3.2720
-15.0	3.0249	2.9828	3.0623	3.0103	3.1003	3.0482	3.2469	3.2348
-14.0	2.9818	2.9397	3.0183	2.9633	3.0546	3.0026	3.2084	3.1953
-13.0	2.9375	2.8954	2.9661	2.9141	3.0069	2.9548	3.1684	3.1563
-12.0	2.8919	2.8498	2.9145	2.8625	2.9568	2.9047	3.1269	3.0749
-11.0	2.8452	2.8647	2.8602	2.8697	2.9041	2.8521	3.0838	3.0317
-10.0	2.7974	2.8169	2.8029	2.8125	2.8485	2.8581	3.0388	2.9868
-9.0	2.7486	2.7681	2.7424	2.7520	2.7899	2.7995	2.9920	2.9400
-8.0	2.6991	2.7186	2.6783	2.6879	2.7277	2.7372	2.9431	2.8910
-7.0	2.6492	2.6687	2.6102	2.6198	2.6615	2.6711	2.8919	2.8399
-6.0	2.5992	2.6188	2.5376	2.5472	2.5909	2.6005	2.8384	2.8480
-5.0	2.5499	2.5695	2.4600	2.4696	2.5152	2.5248	2.7823	2.7918
-4.0	2.5020	2.5215	2.3768	2.3864	2.4338	2.4434	2.7234	2.7330
-3.0	2.4563	2.4759	2.2874	2.2969	2.3457	2.3553	2.6615	2.6711
-2.0	2.4142	2.4337	2.1910	2.2006	2.2499	2.2595	2.5965	2.6061
-1.0	2.3768	2.3963	2.0872	2.0968	2.1452	2.1548	2.5281	2.5377
0.0	2.3457	2.3652	1.9756	1.9852	2.0302	2.0398	2.4563	2.4659
1.0	2.3222	2.3417	1.8566	1.8664	1.9033	1.9129	2.3811	2.3907
2.0	2.3076	2.3271	1.7329	1.7425	1.7632	1.7728	2.3026	2.3122
3.0	2.3026	2.3221	1.6094	1.6190	1.6094	1.6190	2.2213	2.2309
4.0	2.3076	2.3271	1.4979	1.5075	1.4452	1.4548	2.1383	2.1479
5.0	2.3222	2.3417	1.4166	1.4262	1.2825	1.2921	2.0554	2.0650
6.0	2.3457	2.3652	1.3863	1.3959	1.1513	1.1609	1.9756	1.9852
7.0	2.3768	2.3963	1.4166	1.4262	1.0986	1.1082	1.9033	1.9129
8.0	2.4142	2.4337	1.4979	1.5075	1.1513	1.1609	1.8444	1.8540
9.0	2.4563	2.4759	1.6094	1.6190	1.2825	1.2921	1.8055	1.8151
10.0	2.5020	2.5215	1.7329	1.7425	1.4452	1.4548	1.7918	1.8014
11.0	2.5499	2.5695	1.8568	1.8664	1.6094	1.6190	1.8055	1.8151
12.0	2.5992	2.6188	1.9756	1.9852	1.7632	1.7728	1.8444	1.8540
13.0	2.6492	2.6687	2.0872	2.0968	1.9033	1.9129	1.9033	1.9129
14.0	2.6991	2.7186	2.1910	2.2006	2.0302	2.0398	1.9756	1.9852
15.0	2.7486	2.7681	2.2874	2.2969	2.1452	2.1548	2.0554	2.0650
16.0	2.7974	2.8169	2.3768	2.3864	2.2499	2.2595	2.1383	2.1479
17.0	2.8452	2.8647	2.4600	2.4696	2.3457	2.3553	2.2213	2.2309
18.0	2.8919	2.8498	2.5376	2.5472	2.4338	2.4434	2.3026	2.3122
19.0	2.9375	2.8954	2.6102	2.6198	2.5152	2.5248	2.3811	2.3907
20.0	2.9818	2.9397	2.6783	2.6879	2.5909	2.6005	2.4563	2.4659
30.0	3.3601	3.3580	3.1918	3.1797	3.1439	3.0919	3.0388	2.9868
40.0	3.6462	3.6266	3.5332	3.5236	3.5006	3.4910	3.4208	3.4112
50.0	3.8723	3.8494	3.7883	3.7626	3.7636	3.7380	3.7000	3.6705
60.0	4.0582	4.0493	3.9917	3.9729	3.9719	3.9530	3.9192	3.8863
70.0	4.2157	4.1984	4.1608	4.1503	4.1443	4.1338	4.0993	4.0888
80.0	4.3522	4.3627	4.3055	4.2860	4.2913	4.2718	4.2522	4.2249
90.0	4.4725	4.4946	4.4319	4.4442	4.4195	4.4317	4.3848	4.3854
100.0	4.5600	4.5687	4.5442	4.5371	4.5331	4.5260	4.5020	4.4949

Table 11. Computer function generation

MF2(S)	EXPF2(S)	MF3(S)	EXPF3(S)	MF4(S)	EXPF4(S)	CAL. TRS	EXP. TRS	ERROR
3,2698	3,2577	3,3020	3,2899	3,4208	3,4112	.7938	.7997	-.7
3,2315	3,2194	3,2647	3,2526	3,3683	3,3787	.7894	.7953	-.7
3,1918	3,1797	3,2260	3,2139	3,3547	3,3426	.7849	.7617	3.0
3,1504	3,0984	3,1858	3,1737	3,3199	3,3079	.7803	.7276	6.8
3,1073	3,0553	3,1439	3,0919	3,2840	3,2720	.7757	.7528	3.0
3,0623	3,0103	3,1003	3,0482	3,2469	3,2348	.7711	.7483	3.0
3,0153	2,9633	3,0546	3,0026	3,2084	3,1963	.7665	.7439	3.0
2,9661	2,9141	3,0069	2,9548	3,1684	3,1563	.7621	.7396	3.0
2,9145	2,8525	2,9568	2,9047	3,1269	3,0749	.7578	.7354	-1.0
2,8602	2,8697	2,9041	2,8521	3,0838	3,0317	.7539	.8613	-14.2
2,8029	2,8125	2,8485	2,8581	3,0388	2,9868	.7504	.8061	-7.4
2,7424	2,7520	2,7899	2,7995	2,9920	2,9400	.7476	.8031	-7.4
2,6783	2,6879	2,7277	2,7372	2,9431	2,8910	.7458	.8011	-7.4
2,6102	2,6198	2,6615	2,6711	2,8919	2,8399	.7452	.8005	-7.4
2,5376	2,5472	2,5909	2,6005	2,8384	2,8480	.7464	.7539	-1.0
2,4600	2,4696	2,5152	2,5248	2,7823	2,7918	.7501	.7576	-1.0
2,3768	2,3864	2,4338	2,4434	2,7234	2,7330	.7570	.7646	-1.0
2,2874	2,2969	2,3467	2,3553	2,6615	2,6711	.7684	.7760	-1.0
2,1910	2,2006	2,2499	2,2595	2,5965	2,6061	.7857	.7935	-1.0
2,0872	2,0968	2,1452	2,1548	2,5281	2,5377	.8111	.8192	-1.0
1,9756	1,9852	2,0302	2,0398	2,4563	2,4659	.8477	.8561	-1.0
1,8568	1,8664	1,9033	1,9129	2,3811	2,3907	.8999	.9089	-1.0
1,7329	1,7425	1,7632	1,7728	2,3026	2,3122	.9750	.9647	-1.0
1,6094	1,6190	1,6094	1,6190	2,2213	2,2309	1,0847	1,0055	-1.0
1,4979	1,5075	1,4452	1,4548	2,1383	2,1479	1,2485	1,2609	-1.0
1,4166	1,4262	1,2825	1,2921	2,0554	2,0650	1,4932	1,5081	-1.0
1,3863	1,3959	1,1513	1,1609	1,9756	1,9852	1,8314	1,8496	-1.0
1,4166	1,4262	1,0986	1,1082	1,9033	1,9129	2,2066	2,2286	-1.0
1,4979	1,5075	1,1513	1,1609	1,8444	1,8540	2,5000	2,5250	-1.0
1,6094	1,6190	1,2625	1,2921	1,8055	1,8151	2,6587	2,6852	-1.0
1,7329	1,7425	1,4452	1,4548	1,7918	1,8014	2,7126	2,7396	-1.0
1,8568	1,8664	1,6094	1,6190	1,8055	1,8151	2,6961	2,7230	-1.0
1,9756	1,9852	1,7632	1,7728	1,8444	1,8540	2,6307	2,6570	-1.0
2,0872	2,0968	1,9033	1,9129	1,9033	1,9129	2,6337	2,6590	-1.0
2,1910	2,2006	2,0302	2,0398	1,9756	1,9852	2,4212	2,4453	-1.0
2,2874	2,2969	2,1452	2,1548	2,0554	2,0650	2,3054	2,3285	-1.0
2,3768	2,3864	2,2499	2,2595	2,1383	2,1479	2,1944	2,2163	-1.0
2,4600	2,4696	2,3457	2,3553	2,2213	2,2309	2,0921	2,1130	-1.0
2,5376	2,5472	2,4338	2,4434	2,3026	2,3122	2,0000	1,8993	5.0
2,6102	2,6198	2,5152	2,5248	2,3811	2,3907	1,9181	1,8215	5.0
2,6783	2,6879	2,5909	2,6005	2,4563	2,4659	1,8457	1,7528	5.0
3,1918	3,1797	3,1439	3,0919	3,0388	2,9868	1,4465	1,5824	-9.4
3,5332	3,5236	3,5006	3,4910	3,4208	3,4112	1,2943	1,2818	1.0
3,7883	3,7626	3,7636	3,7380	3,7000	3,6705	1,2177	1,2257	-.7
3,9917	3,9729	3,9719	3,9530	3,9192	3,8863	1,1722	1,2006	-2.4
4,1608	4,1503	4,1443	4,1338	4,0993	4,0888	1,1422	1,1344	.7
4,3055	4,2860	4,2913	4,2718	4,2522	4,2249	1,1210	1,1642	-3.9
4,4319	4,4442	4,4195	4,4317	4,3848	4,3854	1,1053	1,1294	-2.2
4,5442	4,5371	4,5331	4,5260	4,5020	4,4949	1,0931	1,1105	-1.6

All experimental points are then computed in the same manner using these constants as

$$EXP = K_2 EXP(\text{nearest } m) + K_1 \text{ remainder} - EXP 1 + K_3 .$$

The $F(s)$ and the $EXP F(s)$ are then computed and listed as CAL.TRS and EXP.TRS, respectively, in Table 11. The final column lists the percentage error between the two. Investigation reveals that the excessive error points are a result of the readings at contact three of the data which is well above all others in error content.

IV. FUNCTION GENERATOR EXPERIMENTS

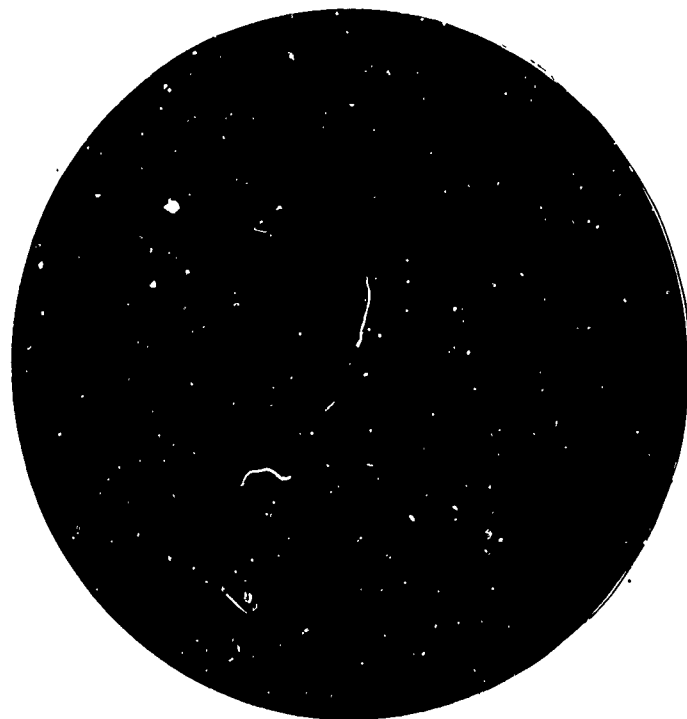
An experiment was made with three sample wafers of the type illustrated in Figure 17. The data for each sample are given in Tables 12 through 14. The same method of fit to an idealized curve as used in part III produced the respective error for wafers 1 and 3.

Wafer 2 indicated two poor data points at 1 and 3. Raw recording indicated interruption during start (point 1) and reading at point 3.

Comparison of data with samples one and three together with corrected data on two would indicate the outcome to be remarkable for reproduction and accuracy.

$$F(s) = \frac{(S + 10 - j3)(S + 4 - j6)}{(S - 3 - j7)(S + 6 - j10)}$$

was again used with the program in Table 15 to produce Tables 16 through 18 for wafers 1 through 3, respectively. The error column reflects the percentage error between the calculated and extrapolated experimental readings. The accuracy is well above that determined as a goal in early stages.



Reproduced from
best available copy.

Figure 17. Wafer 1 of the function generator experiments.

Table 12. Function generator results, wafer 1

Point	Reading	$K_1 (\ln Pt + \ln m)^*$	Error (percent)
1	3.126	3.126	0
2	4.191	4.191	0
3	4.832	4.814	0.4
4	5.259	5.256	0.06
5	4.476	5.599	0.4
6	5.848	5.879	0.5
7	6.107	6.116	0.1
8	6.298	6.321	0.4
9	6.481	6.502	0.3
10	6.625	6.664	0.6
11	6.782	6.810	0.4
12	6.910	6.944	0.5
13	7.043	7.067	0.3
14	7.150	7.181	0.4
15	7.250	7.286	0.5
16	7.353	7.386	0.4
17	7.454	7.479	0.3

* $K_1 = 1.5365$

$\ln m = 2.03$

Table 13. Function generator results, wafer 2

Point	Reading	Calculation 1 and 2*	Error (percent)	Calculation 2 and 4**	Error (percent)
1	3.126	3.126	0	3.100	0.8
2	4.153	4.153	0	4.153	0
3	4.803	4.754	1.0	4.769	0.7
4	5.206	5.180	0.5	5.264	0
5	5.536	5.510	0.5	5.545	0.2
6	5.806	5.781	0.4	5.822	0.3
7	6.065	6.014	0.8	6.056	0.1
8	6.236	6.207	0.5	6.259	0.4
9	6.422	6.381	0.6	6.438	0.2
10	6.585	6.537	0.7	6.598	0.2
11	6.725	6.679	0.7	6.743	0.3
12	6.867	6.808	0.8	6.875	0.1
13	6.983	6.926	0.8	6.996	0.2
14	7.090	7.036	0.8	7.109	0.3
15	7.193	7.138	0.7	7.214	0.3
16	7.284	7.234	0.7	7.312	0.4
17	7.399	7.323	1.0	7.404	0.07

$$*K_1 = 1.4816 \quad \ln m = 2.109822$$

$$**K_1 = 1.519151 \quad \ln m = 2.040614$$

Table 14. Function generator results, wafer 3

Point	Reading	Calculation*	Error (percent)
1	3.126	3.126	0
2	4.193	4.193	0
3	4.819	4.817	0.04
4	5.255	5.260	0.09
5	5.576	5.603	0.5
6	5.861	5.884	0.4
7	6.110	6.121	0.2
8	6.298	6.327	0.5
9	6.483	6.508	0.4
10	6.657	6.670	0.2
11	6.798	6.817	0.3
12	6.928	6.951	0.3
13	7.053	7.074	0.3
14	7.169	7.188	0.3
15	7.268	7.294	0.4
16	7.369	7.394	0.3
17	7.464	7.487	0.3

* $K_1 = 1.5393$ $\ln m = 2.0307$

Table 15. Final function generator program

PROGRAM	TRANSF
	PROGRAM TRANSF(INPUT,OUTPUT)
	C EVALUATION OF BROWN TRANSFER FUNCTION NO. 2
	C TRAN. FUNC. $= (S-10+J3)(S-4+J6)/(S+3+J7)(S-6+J10)$
5	COMPLEX FU(4),FC(4),S,TFC0,TFC1,TFC13,TFC40 REAL FMAG(4),FLOG(4),FTRSF,FRFQ,EXPMF(4),CK2(4),CK3(4),VEXP(17) READ 2,FU
	2 FORMAT(8F6.1)
	DO 20 L=1,3
	READ 1,CK1,IO
10	1 FORMAT(6X,F10.4,15X,A2)
	PRINT 6,IO,CK1
	6 FORMAT(1H1,4X10HWAFFER IO =,A2,10X7HK1=,F10.4/)
	DO 4 I=1,17
	READ 3, FPOS
15	3 FORMAT(5X,F10.3)
	4 VEXP(I)=FPOS
	S=(0.0,-?0.0)
	C FIND VALUES OF CONSTANTS
	DO 9 N=1,4
20	TFC0=FU(N)
	TFC1=(0.0,1.0)+FU(N)
	TFC13=(0.0,13.0)+FU(N)
	TFC40=(0.0,40.0)+FU(N)
	TFM0=CA7S(TFC0)
25	TFM1=CA0S(TFC1)
	TFM13=CA3S(TFC13)
	TFM40=CA7S(TFC40)
	TFLN0=ALOG(TFM0)
	TFLN1=ALOG(TFM1)
30	TFLN13=ALOG(TFM13)
	TFLN40=ALOG(TFM40)
	TOFL0=0.17*TFM0
	TOFL1=0.17*TFM1
	TOFL13=0.17*TFM13
35	TOFL40=0.17*TFM40
	IOIS0=INT(TOFL0)
	IOIS1=INT(TOFL1)
	IOIS13=INT(TOFL13)
	IOIS40=INT(TOFL40)
40	RFM0=TOEL0/FLOAT(IOIS0)
	RFM1=TOEL1/FLOAT(IOIS1)
	RFM13=TOEL13/FLOAT(IOIS13)
	RFM40=TOEL40/FLOAT(IOIS40)
	VAL0=VEXP(IOIS0)+CK1*ALOG(RFM0)
45	VAL1=VEXP(IOIS1)+CK1*ALOG(RFM1)
	VAL13=VEXP(IOIS13)+CK1*ALOG(RFM13)
	VAL40=VEXP(IOIS40)+CK1*ALOG(RFM40)
	CK2(N)=(TFLN1-TFLN0)/(VAL1-VAL0)
	TFM0A=TFLN0-(VAL40-VEXP(1))*CK2(N)
50	TFM0B=TFLN13-(VAL13-VEXP(1))*CK2(N)
	CK3(N)=(TFM0A+TFM0B)/2.0
	PRINT 999,CK2(N),CK3(N)
	999 FORMAT(20X,2F10.4)
	9 CONTINUE
55	PRINT 5

Reproduced from
best available copy.

Table 15. (continued)

PROGRAM	TRANSF
	<pre> 5 FORMAT(1H0,2X113HF0 MF1(S) FXPF1(S) MF2(S) EXPF2(S) XMF3(S) EXPF3(S) MF4(S) EXPF4(S) CAL.TRS EXP.TRS ERPR/1 C EVALUATE COMPLEX FUNCTION,MODULUS,AND NATURAL LOG. DO 20 I=1,49 60 DO 17 J=1,4 FC(J)=S+FU(J) FMAG(J)=CABS(FC(J)) FLOG(J)=ALOG(FMAG(J)) DFLR=0.17*FMAG(J) 65 IDIST=INT(DFLR) IF(IDIST.FQ.0) IDIST=1 RFMX=DFLR/DFLR(IDIST) VAL2=VEXP(IDIST)+CK1*ALOG(RFMX) FXPMF(J)=CK2(J)*(VAL2-VEXP(1))+CK3(J) 70 17 CONTINUE C EVALUATE TRANSFER FUNCTION FTRSF=FLOG(1)+G(2)-FLOG(3)-FLOG(4) FXPTR=FXPMF(1)+FXPMF(2)-FXPMF(3)-FXPMF(4) VTRSF=EXP(FTRSF) VXPTR=EXP(FXPTR) 75 ERPR=((VTRSF-VXPTR)/VTRSF)*100.0 FRFQ=AIMAG(S) PPINT 99,FRFQ,(FLOG(K),FXPMF(K) ,K=1,4),VTRSF,VXPTR,ERPR 80 99 FORMAT(2X,F6.1,10F10.4,F9.1) IF(I.GE.41) GO TO 19 S=S+(0.0,1.0) GO TO 20 19 S=S+(0.0,10.0) 20 CONTINUE 85 END </pre>

Reproduced from
best available copy.

Table 16. Computer function generation, wafer 1

K1= 1.5365								
FREQ	MF1(S)	FXPF1(S)	MF2(S)	FXPF2(S)	MF3(S)	FXPF3(S)	MF4(S)	FXPF4(S)
-20.0	3.2221	3.2341	3.2698	3.2792	3.3020	3.3113	3.4208	3.4134
-19.0	3.1850	3.1970	3.2315	3.2409	3.2647	3.2741	3.3883	3.3808
-18.0	3.1467	3.1685	3.1918	3.2011	3.2260	3.2354	3.3547	3.3640
-17.0	3.1073	3.1291	3.1504	3.1695	3.1858	3.1952	3.3199	3.3293
-16.0	3.0667	3.0885	3.1073	3.1265	3.1439	3.1631	3.2840	3.2934
-15.0	3.0249	3.0467	3.0623	3.0815	3.1003	3.1194	3.2469	3.2563
-14.0	2.9818	3.0036	3.0153	3.0345	3.0546	3.0738	3.2084	3.2177
-13.0	2.9375	2.9593	2.9661	2.9853	3.0069	3.0260	3.1684	3.1778
-12.0	2.8919	2.9137	2.9145	2.9336	2.9568	2.9759	3.1269	3.1461
-11.0	2.8452	2.8553	2.8602	2.8676	2.9041	2.9232	3.0838	3.1029
-10.0	2.7974	2.8074	2.8029	2.8103	2.8485	2.8560	3.0388	3.0580
-9.0	2.7486	2.7587	2.7424	2.7498	2.7899	2.7973	2.9920	3.0111
-8.0	2.6991	2.7092	2.6783	2.6857	2.7277	2.7351	2.9431	2.9622
-7.0	2.6492	2.6593	2.6102	2.6176	2.6615	2.6689	2.8919	2.9111
-6.0	2.5992	2.6093	2.5376	2.5450	2.5909	2.5983	2.8384	2.8458
-5.0	2.5499	2.5600	2.4630	2.4674	2.5152	2.5227	2.7823	2.7897
-4.0	2.5020	2.5121	2.3768	2.3842	2.4338	2.4412	2.7234	2.7308
-3.0	2.4563	2.4664	2.2874	2.2948	2.3457	2.3531	2.6615	2.6689
-2.0	2.4142	2.4243	2.1910	2.1985	2.2499	2.2574	2.5965	2.6039
-1.0	2.3768	2.3869	2.0872	2.0946	2.1452	2.1527	2.5281	2.5356
0.0	2.3457	2.3558	1.9756	1.9831	2.0302	2.0377	2.4553	2.4638
1.0	2.3222	2.3323	1.8568	1.8642	1.9033	1.9108	2.3811	2.3885
2.0	2.3076	2.3177	1.7329	1.7403	1.7632	1.7706	2.3026	2.3100
3.0	2.3026	2.3127	1.6094	1.6169	1.6094	1.6169	2.2213	2.2288
4.0	2.3076	2.3177	1.4979	1.5053	1.4452	1.4526	2.1383	2.1458
5.0	2.3222	2.3323	1.4166	1.4241	1.2825	1.2899	2.0554	2.0629
6.0	2.3457	2.3558	1.3863	1.3937	1.1513	1.1587	1.9756	1.9831
7.0	2.3768	2.3869	1.4166	1.4241	1.0986	1.1061	1.9033	1.9108
8.0	2.4142	2.4243	1.4979	1.5053	1.1513	1.1587	1.8444	1.8519
9.0	2.4563	2.4664	1.6094	1.6169	1.2825	1.2899	1.8055	1.8129
10.0	2.5020	2.5121	1.7329	1.7403	1.4452	1.4526	1.7918	1.7992
11.0	2.5499	2.5600	1.8568	1.8642	1.6094	1.6169	1.8055	1.8129
12.0	2.5992	2.6093	1.9756	1.9831	1.7632	1.7706	1.8444	1.8519
13.0	2.6492	2.6593	2.0872	2.0946	1.9033	1.9108	1.9033	1.9108
14.0	2.6991	2.7092	2.1910	2.1985	2.0302	2.0377	1.9756	1.9831
15.0	2.7486	2.7587	2.2874	2.2948	2.1452	2.1527	2.0554	2.0629
16.0	2.7974	2.8074	2.3768	2.3842	2.2499	2.2574	2.1383	2.1458
17.0	2.8452	2.8553	2.4600	2.4674	2.3457	2.3531	2.2213	2.2288
18.0	2.8919	2.9137	2.5376	2.5450	2.4338	2.4412	2.3026	2.3100
19.0	2.9375	2.9593	2.6102	2.6176	2.5152	2.5227	2.3811	2.3885
20.0	2.9818	3.0036	2.6783	2.6857	2.5909	2.5983	2.4563	2.4638
30.0	3.3601	3.3721	3.1918	3.2011	3.1439	3.1631	3.0388	3.0580
40.0	3.6462	3.6361	3.5332	3.5258	3.5106	3.4932	3.4208	3.4134
50.0	3.8723	3.8674	3.7883	3.7900	3.7636	3.7553	3.7000	3.6873
60.0	4.0582	4.0546	3.9917	3.9855	3.9719	3.9657	3.9192	3.9116
70.0	4.2157	4.2074	4.1608	4.1430	4.1443	4.1264	4.0993	4.0814
80.0	4.3522	4.3466	4.3055	4.2908	4.2913	4.2766	4.2522	4.2411
90.0	4.4725	4.4625	4.4319	4.4193	4.4195	4.4068	4.3848	4.3766
100.0	4.5800	4.5686	4.5442	4.5276	4.5331	4.5165	4.5020	4.4855

Table 16. Computer function generation, wafer 1

1.5365								
MF2(S)	FXPF2(S)	MF3(S)	FXPF3(S)	MF4(S)	FXPF4(S)	CAL.TRS	FXP.TRS	ERROR
3.2698	3.2792	3.3020	3.3113	3.4208	3.4134	.7938	.8094	-2.0
3.2315	3.2409	3.2647	3.2741	3.3883	3.3808	.7894	.8049	-2.0
3.1918	3.2011	3.2260	3.2354	3.3547	3.3640	.7849	.7947	-1.3
3.1504	3.1695	3.1858	3.1952	3.3199	3.3293	.7803	.7978	-2.2
3.1073	3.1265	3.1439	3.1631	3.2840	3.2934	.7757	.7854	-1.3
3.0623	3.0815	3.1003	3.1194	3.2469	3.2563	.7711	.7808	-1.3
3.0153	3.0345	3.0546	3.0738	3.2084	3.2177	.7665	.7761	-1.3
2.9661	2.9853	3.0069	3.0260	3.1584	3.1778	.7621	.7716	-1.3
2.9145	2.9336	2.9568	2.9759	3.1269	3.1461	.7578	.7599	-.3
2.8602	2.8676	2.9041	2.9232	3.0838	3.1029	.7539	.7384	2.1
2.8029	2.8103	2.8485	2.8560	3.0388	3.0580	.7504	.7437	.9
2.7424	2.7498	2.7899	2.7973	2.9920	3.0111	.7476	.7409	.9
2.6783	2.6857	2.7277	2.7351	2.9431	2.9622	.7458	.7390	.9
2.6102	2.6176	2.6615	2.6689	2.8919	2.9111	.7452	.7385	.9
2.5376	2.5450	2.5909	2.5983	2.8384	2.8458	.7464	.7484	-.3
2.4600	2.4674	2.5152	2.5227	2.7823	2.7897	.7501	.7521	-.3
2.3768	2.3842	2.4338	2.4412	2.7234	2.7308	.7570	.7590	-.3
2.2874	2.2948	2.3457	2.3531	2.6615	2.6689	.7684	.7704	-.3
2.1910	2.1985	2.2499	2.2574	2.5965	2.6039	.7857	.7878	-.3
2.0872	2.0946	2.1452	2.1527	2.5281	2.5356	.8111	.8133	-.3
1.9756	1.9831	2.0302	2.0377	2.4553	2.4638	.8477	.8499	-.3
1.8568	1.8642	1.9033	1.9108	2.3811	2.3885	.8999	.9023	-.3
1.7329	1.7403	1.7632	1.7706	2.3026	2.3100	.9750	.9776	-.3
1.6094	1.6169	1.6094	1.6169	2.2213	2.2288	1.0847	1.0875	-.3
1.4979	1.5053	1.4452	1.4526	2.1383	2.1458	1.2485	1.2518	-.3
1.4166	1.4241	1.2825	1.2899	2.0554	2.0629	1.4932	1.4971	-.3
1.3863	1.3937	1.1513	1.1587	1.9756	1.9831	1.0314	1.0362	-.3
1.4166	1.4241	1.0986	1.1061	1.9033	1.9108	2.2066	2.2125	-.3
1.4979	1.5053	1.1513	1.1587	1.8444	1.8519	2.5000	2.5066	-.3
1.6094	1.6169	1.2825	1.2899	1.8055	1.8129	2.6587	2.6658	-.3
1.7329	1.7403	1.4452	1.4526	1.7918	1.7992	2.7126	2.7197	-.3
1.8568	1.8642	1.6094	1.6169	1.8055	1.8129	2.6961	2.7033	-.3
1.9756	1.9831	1.7632	1.7706	1.8444	1.8519	2.6307	2.6377	-.3
2.0872	2.0946	1.9033	1.9108	1.9033	1.9108	2.5337	2.5404	-.3
2.1910	2.1985	2.0302	2.0377	1.9756	1.9831	2.4212	2.4276	-.3
2.2874	2.2948	2.1452	2.1527	2.0554	2.0629	2.3054	2.3115	-.3
2.3768	2.3842	2.2499	2.2574	2.1383	2.1458	2.1944	2.2002	-.3
2.4600	2.4674	2.3457	2.3531	2.2213	2.2288	2.0921	2.0976	-.3
2.5376	2.5450	2.4338	2.4412	2.3026	2.3100	2.0000	2.0289	-1.4
2.6102	2.6176	2.5152	2.5227	2.3811	2.3885	1.9181	1.9458	-1.4
2.6783	2.6857	2.5909	2.5983	2.4563	2.4638	1.8457	1.8724	-1.4
3.1918	3.2011	3.1439	3.1631	3.0388	3.0580	1.4465	1.4222	1.7
3.5332	3.5258	3.5006	3.4932	3.4208	3.4134	1.2943	1.2909	.3
3.7683	3.7900	3.7636	3.7653	3.7000	3.6873	1.2177	1.2273	-.8
3.9917	3.9855	3.9719	3.9657	3.9192	3.9116	1.1722	1.1768	-.4
4.1508	4.1430	4.1443	4.1264	4.0993	4.0814	1.1422	1.1531	-1.0
4.3055	4.2908	4.2913	4.2766	4.2522	4.2411	1.1210	1.1272	-.5
4.4319	4.4193	4.4195	4.4068	4.3848	4.3766	1.1053	1.1033	.2
4.5442	4.5276	4.5331	4.5165	4.5020	4.4855	1.0931	1.0988	-.5

Table 17. Computer function generation, wave ?

K1= 1.5192									
FREQ	MF1(S)	FXPF1(S)	MF2(S)	FXPF2(S)	MF3(S)	EXPF3(S)	MF4(S)	FXPF4(S)	CAL. TRS
-20.0	3.2221	3.2273	3.2699	3.2727	3.3020	3.3049	3.4209	3.4179	.7938
-19.0	3.1850	3.1902	3.2315	3.2345	3.2647	3.2677	3.3883	3.3853	.7894
-18.0	3.1467	3.1744	3.1918	3.1947	3.2260	3.2290	3.3547	3.3576	.7849
-17.0	3.1073	3.1350	3.1504	3.1757	3.1858	3.1887	3.3199	3.3229	.7803
-16.0	3.0667	3.0944	3.1073	3.1327	3.1439	3.1693	3.2840	3.2870	.7757
-15.0	3.0249	3.0525	3.0623	3.0877	3.1003	3.1256	3.2469	3.2498	.7711
-14.0	2.9818	3.0095	3.0153	3.0407	3.0546	3.0800	3.2084	3.2113	.7665
-13.0	2.9375	2.9651	2.9661	2.9915	3.0069	3.0322	3.1684	3.1714	.7621
-12.0	2.8919	2.9196	2.9145	2.9398	2.9568	2.9821	3.1269	3.1523	.7578
-11.0	2.8452	2.8504	2.8602	2.8631	2.9041	2.9294	3.0938	3.1091	.7539
-10.0	2.7974	2.8026	2.8029	2.8059	2.8485	2.8515	3.0388	3.0642	.7504
-9.0	2.7486	2.7539	2.7424	2.7454	2.7899	2.7928	2.9920	3.0173	.7476
-8.0	2.6991	2.7044	2.6783	2.6813	2.7277	2.7306	2.9431	2.9684	.7458
-7.0	2.6492	2.6544	2.6102	2.6131	2.6615	2.6645	2.8919	2.9173	.7452
-6.0	2.5992	2.6045	2.5376	2.5405	2.5909	2.5939	2.8384	2.8413	.7464
-5.0	2.5499	2.5552	2.4600	2.4630	2.5152	2.5182	2.7823	2.7852	.7501
-4.0	2.5020	2.5072	2.3768	2.3798	2.4338	2.4367	2.7234	2.7263	.7570
-3.0	2.4563	2.4616	2.2874	2.2903	2.3457	2.3487	2.6615	2.6645	.7684
-2.0	2.4142	2.4194	2.1910	2.1940	2.2499	2.2529	2.5965	2.5994	.7857
-1.0	2.3768	2.3821	2.0872	2.0902	2.1452	2.1482	2.5281	2.5311	.8111
0.0	2.3457	2.3510	1.9756	1.9786	2.0302	2.0332	2.4563	2.4593	.8477
1.0	2.3222	2.3275	1.8568	1.8598	1.9033	1.9063	2.3811	2.3841	.8999
2.0	2.3076	2.3128	1.7329	1.7358	1.7632	1.7662	2.3026	2.3056	.9750
3.0	2.3026	2.3079	1.6094	1.6124	1.6094	1.6124	2.2213	2.2243	1.0847
4.0	2.3076	2.3128	1.4979	1.5008	1.4452	1.4482	2.1383	2.1413	1.2455
5.0	2.3222	2.3275	1.4166	1.4196	1.2825	1.2855	2.0554	2.0584	1.4932
6.0	2.3457	2.3510	1.3863	1.3893	1.1513	1.1543	1.9756	1.9786	1.8314
7.0	2.3768	2.3821	1.4166	1.4196	1.0986	1.1016	1.9033	1.9063	2.2066
8.0	2.4142	2.4194	1.4979	1.5008	1.1513	1.1543	1.8444	1.8474	2.5000
9.0	2.4563	2.4616	1.6034	1.6124	1.2825	1.2855	1.8055	1.8084	2.6587
10.0	2.5020	2.5072	1.7329	1.7358	1.4452	1.4482	1.7918	1.7947	2.7126
11.0	2.5499	2.5552	1.8568	1.8598	1.6094	1.6124	1.8055	1.8084	2.6961
12.0	2.5992	2.6045	1.9756	1.9786	1.7632	1.7662	1.8444	1.8474	2.6307
13.0	2.6492	2.6544	2.0872	2.0902	1.9033	1.9063	1.9033	1.9063	2.5337
14.0	2.6991	2.7044	2.1910	2.1940	2.0302	2.0332	1.9756	1.9786	2.4212
15.0	2.7486	2.7539	2.2874	2.2903	2.1452	2.1482	2.0554	2.0584	2.3054
16.0	2.7974	2.8026	2.3768	2.3798	2.2499	2.2529	2.1383	2.1413	2.1944
17.0	2.8452	2.8504	2.4600	2.4630	2.3457	2.3487	2.2213	2.2243	2.0921
18.0	2.8919	2.9196	2.5376	2.5405	2.4338	2.4367	2.3026	2.3056	2.0000
19.0	2.9375	2.9651	2.6102	2.6131	2.5152	2.5182	2.3811	2.3841	1.9181
20.0	2.9818	3.0095	2.6783	2.6813	2.5909	2.5939	2.4563	2.4593	1.8457
30.0	3.3601	3.3654	3.1918	3.1947	3.1439	3.1693	3.0388	3.0642	1.4465
40.0	3.6462	3.6409	3.5332	3.5303	3.5006	3.4976	3.4208	3.4178	1.2943
50.0	3.8723	3.8624	3.7883	4.1525	3.7636	4.1278	3.7000	3.6924	1.2177
60.0	4.0582	4.0530	3.9917	3.9842	3.9719	3.9643	3.9192	3.9070	1.1722
70.0	4.2157	4.2052	4.1608	4.1552	4.1443	4.1386	4.0993	4.0937	1.1422
80.0	4.3522	4.3485	4.3055	4.3032	4.2913	4.2890	4.2522	4.2434	1.1210
90.0	4.4725	4.4651	4.4319	4.4223	4.4195	4.4098	4.3848	4.3788	1.1053
100.0	4.5800	4.5668	4.5442	4.5333	4.5331	4.5222	4.5020	4.4911	1.0931

Table 17. Computer function generation, wafers

K1= 1.5192									
F1(S)	MF2(S)	FXPF2(S)	MF3(S)	EXPF3(S)	MF4(S)	FXPF4(S)	CAL.TRS	FXP.TRS	ERROR
2273	3.2699	3.2727	3.3020	3.3049	3.4208	3.4178	.7938	.8004	-.8
1902	3.2315	3.2345	3.2647	3.2677	3.3883	3.3853	.7894	.7959	-.8
1744	3.1914	3.1947	3.2260	3.2290	3.3547	3.3576	.7849	.8045	-2.5
1350	3.1504	3.1757	3.1858	3.1887	3.3199	3.3229	.7803	.8180	-4.8
0944	3.1073	3.1327	3.1439	3.1693	3.2840	3.2870	.7757	.7951	-2.5
0525	3.0623	3.0877	3.1003	3.1256	3.2469	3.2498	.7711	.7904	-2.5
0095	3.0153	3.0407	3.0546	3.0800	3.2084	3.2113	.7665	.7857	-2.5
9651	2.9661	2.9915	3.0069	3.0322	3.1684	3.1714	.7621	.7812	-2.5
9196	2.9145	2.9398	2.9568	2.9821	3.1269	3.1523	.7578	.7596	-.2
8504	2.8602	2.8631	2.9041	2.9294	3.0838	3.1091	.7534	.7225	4.2
8026	2.8029	2.8059	2.8485	2.8515	3.0388	3.0641	.7504	.7355	2.0
7539	2.7424	2.7454	2.7899	2.7928	2.9920	3.0173	.7476	.7328	2.0
7044	2.6783	2.6813	2.7277	2.7306	2.9431	2.9684	.7458	.7309	2.0
6544	2.6102	2.6131	2.6615	2.6645	2.8919	2.9173	.7452	.7304	2.0
6045	2.5376	2.5405	2.5909	2.5939	2.8384	2.8413	.7464	.7482	-.2
5552	2.4600	2.4630	2.5152	2.5182	2.7823	2.7852	.7501	.7518	-.2
5072	2.3768	2.3798	2.4338	2.4367	2.7234	2.7263	.7570	.7588	-.2
4616	2.2874	2.2903	2.3457	2.3487	2.6615	2.6645	.7684	.7702	-.2
4194	2.1910	2.1940	2.2499	2.2529	2.5965	2.5994	.7857	.7875	-.2
3821	2.0872	2.0902	2.1452	2.1482	2.5281	2.5311	.8111	.8130	-.2
3510	1.9756	1.9786	2.0302	2.0332	2.4563	2.4593	.8477	.8496	-.2
3275	1.8568	1.8598	1.9033	1.9063	2.3811	2.3841	.8999	.9020	-.2
3128	1.7329	1.7358	1.7632	1.7662	2.3026	2.3056	.9750	.9772	-.2
3079	1.6094	1.6124	1.6094	1.6124	2.2213	2.2243	1.0847	1.0872	-.2
3128	1.4979	1.5008	1.4452	1.4482	2.1383	2.1413	1.2485	1.2513	-.2
3275	1.4166	1.4196	1.2825	1.2855	2.0554	2.0584	1.4932	1.4966	-.2
3510	1.3863	1.3893	1.1513	1.1543	1.9756	1.9786	1.8314	1.8356	-.2
3821	1.4166	1.4196	1.0946	1.1016	1.9033	1.9063	2.2066	2.2117	-.2
4194	1.4979	1.5008	1.1513	1.1543	1.8444	1.8474	2.5000	2.5058	-.2
4616	1.6034	1.6124	1.2825	1.2855	1.8055	1.8084	2.6587	2.6648	-.2
5072	1.7329	1.7358	1.4452	1.4482	1.7918	1.7947	2.7126	2.7188	-.2
5552	1.8568	1.8598	1.6094	1.6124	1.8055	1.8084	2.6961	2.7023	-.2
6045	1.9756	1.9786	1.7632	1.7662	1.8444	1.8474	2.6307	2.6367	-.2
6544	2.0872	2.0902	1.9033	1.9063	1.9033	1.9063	2.5337	2.5395	-.2
7044	2.1910	2.1940	2.0302	2.0332	1.9756	1.9786	2.4212	2.4267	-.2
7539	2.2874	2.2903	2.1452	2.1482	2.0554	2.0584	2.3054	2.3107	-.2
8026	2.3768	2.3798	2.2499	2.2529	2.1383	2.1413	2.1944	2.1994	-.2
8504	2.4600	2.4630	2.3457	2.3487	2.2213	2.2243	2.0921	2.0969	-.2
9196	2.5376	2.5405	2.4338	2.4367	2.3026	2.3056	2.0000	2.0499	-2.5
9651	2.6102	2.6131	2.5152	2.5182	2.3811	2.3841	1.9181	1.9660	-2.5
0095	2.6783	2.6813	2.5909	2.5939	2.4563	2.4593	1.8457	1.8918	-2.5
3654	3.1918	3.1947	3.1439	3.1693	3.0388	3.0642	1.4465	1.3862	4.2
6409	3.5332	3.5303	3.5906	3.4976	3.4298	3.4178	1.2943	1.2913	.2
8624	3.7883	4.1525	3.7636	4.1278	3.7000	3.6924	1.2177	1.2149	.2
0530	3.9917	3.9842	3.9719	3.9643	3.9192	3.9070	1.1722	1.1804	-.7
2092	4.1608	4.1552	4.1443	4.1386	4.0993	4.0937	1.1422	1.1412	.1
3485	4.3055	4.3032	4.2913	4.2890	4.2522	4.2434	1.1210	1.1267	-.5
4651	4.4319	4.4223	4.4195	4.4098	4.3848	4.3788	1.1053	1.1038	.1
5668	4.5442	4.5333	4.5331	4.5222	4.5020	4.4911	1.0931	1.0906	.2

Table 18. Computer function generation, wafer 3

K1= 1.5393										
FREQ	MF1(S)	FXPF1(S)	MF2(S)	FXPF2(S)	MF3(S)	FXPF3(S)	MF4(S)	FXPF4(S)	CAL.TRS	FXP.
-20.0	3.2221	3.2263	3.2698	3.2755	3.3020	3.3077	3.4208	3.4119	.7938	.
-19.0	3.1850	3.1892	3.2315	3.2372	3.2647	3.2704	3.3883	3.3794	.7894	.
-18.0	3.1467	3.1554	3.1918	3.1975	3.2260	3.2317	3.3547	3.3604	.7849	.
-17.0	3.1073	3.1160	3.1504	3.1605	3.1858	3.1915	3.3199	3.3256	.7803	.
-16.0	3.0667	3.0754	3.1073	3.1174	3.1439	3.1541	3.2840	3.2897	.7757	.
-15.0	3.0249	3.0336	3.0623	3.0725	3.1003	3.1104	3.2469	3.2526	.7711	.
-14.0	2.9818	2.9905	3.0153	3.0255	3.0546	3.0648	3.2084	3.2141	.7665	.
-13.0	2.9375	2.9462	2.9661	2.9763	3.0069	3.0170	3.1684	3.1741	.7621	.
-12.0	2.8919	2.9006	2.9145	2.9246	2.9568	2.9669	3.1269	3.1371	.7578	.
-11.0	2.8452	2.8527	2.8602	2.8691	2.9041	2.9142	3.0838	3.0939	.7539	.
-10.0	2.7974	2.8049	2.8029	2.8118	2.8485	2.8575	3.0388	3.0490	.7504	.
-9.0	2.7486	2.7561	2.7424	2.7513	2.7899	2.7988	2.9920	3.0021	.7476	.
-8.0	2.6991	2.7066	2.6783	2.6872	2.7277	2.7366	2.9431	2.9532	.7458	.
-7.0	2.6492	2.6567	2.6102	2.6191	2.6615	2.6704	2.8919	2.9021	.7452	.
-6.0	2.5992	2.6067	2.5376	2.5465	2.5909	2.5998	2.8384	2.8473	.7464	.
-5.0	2.5499	2.5574	2.4600	2.4689	2.5152	2.5241	2.7823	2.7912	.7501	.
-4.0	2.5020	2.5095	2.3768	2.3857	2.4338	2.4427	2.7234	2.7323	.7570	.
-3.0	2.4563	2.4638	2.2874	2.2963	2.3457	2.3546	2.6615	2.6704	.7684	.
-2.0	2.4142	2.4216	2.1910	2.1999	2.2499	2.2588	2.5965	2.6054	.7857	.
-1.0	2.3768	2.3843	2.0872	2.0961	2.1452	2.1541	2.5281	2.5371	.8111	.
0.0	2.3457	2.3532	1.9756	1.9845	2.0302	2.0391	2.4563	2.4652	.8477	.
1.0	2.3222	2.3297	1.8568	1.8657	1.9033	1.9122	2.3811	2.3900	.8999	.
2.0	2.3076	2.3150	1.7329	1.7418	1.7632	1.7721	2.3026	2.3115	.9750	.
3.0	2.3026	2.3101	1.6094	1.6183	1.6094	1.6183	2.2213	2.2302	1.0847	1.
4.0	2.3076	2.3150	1.4979	1.5068	1.4452	1.4541	2.1383	2.1472	1.2485	1.
5.0	2.3222	2.3297	1.4166	1.4255	1.2825	1.2914	2.0554	2.0643	1.4932	1.
6.0	2.3457	2.3532	1.3863	1.3952	1.1513	1.1602	1.9756	1.9845	1.8314	1.
7.0	2.3768	2.3843	1.4166	1.4255	1.0986	1.1075	1.9033	1.9122	2.2066	2.
8.0	2.4142	2.4216	1.4979	1.5068	1.1513	1.1602	1.8444	1.8533	2.5000	2.
9.0	2.4563	2.4638	1.6094	1.6183	1.2825	1.2914	1.8055	1.8144	2.6587	2.
10.0	2.5020	2.5095	1.7329	1.7418	1.4452	1.4541	1.7911	1.8007	2.7126	2.
11.0	2.5499	2.5574	1.8568	1.8657	1.6094	1.6183	1.8055	1.8144	2.6961	2.
12.0	2.5992	2.6067	1.9756	1.9845	1.7632	1.7721	1.8444	1.8533	2.6307	2.
13.0	2.6492	2.6567	2.0872	2.0961	1.9033	1.9122	1.9033	1.9122	2.5337	2.
14.0	2.6991	2.7066	2.1910	2.1999	2.0302	2.0391	1.9756	1.9845	2.4217	2.
15.0	2.7486	2.7561	2.2874	2.2963	2.1452	2.1541	2.0554	2.0643	2.3054	2.
16.0	2.7974	2.8049	2.3768	2.3857	2.2499	2.2588	2.1383	2.1472	2.1944	2.
17.0	2.8452	2.8527	2.4600	2.4689	2.3457	2.3546	2.2213	2.2302	2.0921	2.
18.0	2.8919	2.9006	2.5376	2.5465	2.4338	2.4427	2.3026	2.3115	2.0000	1.
19.0	2.9375	2.9462	2.6102	2.6191	2.5152	2.5241	2.3811	2.3900	1.9181	1.
20.0	2.9818	2.9905	2.6783	2.6872	2.5909	2.5998	2.4563	2.4652	1.8457	1.
30.0	3.3601	3.3644	3.1918	3.1975	3.1439	3.1541	3.0388	3.0490	1.4465	1.
40.0	3.6462	3.6387	3.5332	3.5244	3.5006	3.4917	3.4208	3.4119	1.2943	1.
50.0	3.8723	3.8610	3.7883	3.7898	3.7636	3.7652	3.7000	3.6939	1.2177	1.
60.0	4.0582	4.0493	3.9917	3.9843	3.9719	3.9644	3.9192	3.9093	1.1722	1.
70.0	4.2157	4.2108	4.1609	4.1610	4.1443	4.1445	4.0993	4.0995	1.1422	1.
80.0	4.3522	4.3459	4.3055	4.2995	4.2913	4.2853	4.2522	4.2487	1.1210	1.
90.0	4.4725	4.4674	4.4319	4.4283	4.4195	4.4159	4.3848	4.3799	1.1053	1.
100.0	4.5800	4.5713	4.5442	4.5359	4.5331	4.5248	4.5020	4.4937	1.0931	1.

Table 18. Computer function generation, wafer 3

	K1= 1.5393									
	FXPF1(S)	MF2(S)	FXPF2(S)	MF3(S)	FXPF3(S)	MF4(S)	FXPF4(S)	CAL.TRS	EXP.TRS	ERROR
1	3.2263	3.2698	3.2755	3.3020	3.3077	3.4208	3.4119	.7938	.8043	-1.3
0	3.1892	3.2315	3.2372	3.2647	3.2704	3.3883	3.3794	.7894	.7999	-1.3
7	3.1554	3.1918	3.1975	3.2260	3.2317	3.3547	3.3604	.7849	.7873	-.3
3	3.1160	3.1504	3.1605	3.1858	3.1915	3.3199	3.3256	.7803	.7862	-.7
7	3.0754	3.1073	3.1174	3.1439	3.1541	3.2840	3.2897	.7757	.7781	-.3
9	3.0336	3.0623	3.0725	3.1003	3.1104	3.2469	3.2526	.7711	.7734	-.3
8	2.9905	3.015	3.0255	3.0546	3.0648	3.2084	3.2141	.7665	.7689	-.3
5	2.9462	2.9661	2.9763	3.0069	3.0170	3.1684	3.1741	.7621	.7644	-.3
9	2.9006	2.9145	2.9246	2.9568	2.9669	3.1269	3.1371	.7578	.7568	.1
2	2.8527	2.8602	2.8691	2.9041	2.9142	3.0838	3.0939	.7539	.7510	.4
4	2.8049	2.8029	2.8118	2.8485	2.8575	3.0388	3.0490	.7504	.7485	.3
6	2.7561	2.7424	2.7513	2.7899	2.7988	2.9920	3.0021	.7476	.7457	.3
1	2.7066	2.6783	2.6872	2.7277	2.7366	2.9431	2.9532	.7458	.7438	.3
2	2.6567	2.6102	2.6191	2.6615	2.6704	2.8919	2.9021	.7452	.7433	.3
2	2.6057	2.5376	2.5465	2.5909	2.5998	2.8384	2.8473	.7464	.7454	.1
9	2.5574	2.4600	2.4689	2.5152	2.5241	2.7823	2.7912	.7501	.7490	.1
0	2.5095	2.3768	2.3857	2.4338	2.4427	2.7234	2.7323	.7570	.7559	.1
3	2.4638	2.2874	2.2963	2.3457	2.3546	2.6615	2.6704	.7634	.7672	.1
2	2.4216	2.1910	2.1999	2.2499	2.2588	2.5965	2.6054	.7857	.7845	.1
8	2.3843	2.0872	2.0961	2.1452	2.1541	2.5281	2.5371	.8111	.8099	.1
7	2.3532	1.9756	1.9845	2.0302	2.0391	2.4563	2.4652	.8477	.8465	.1
2	2.3297	1.8568	1.8657	1.9033	1.9122	2.3811	2.3900	.8999	.8986	.1
3	2.3150	1.7329	1.7418	1.7632	1.7721	2.3026	2.3115	.9750	.9736	.1
2	2.3101	1.6094	1.6183	1.6094	1.6183	2.2213	2.2302	1.0847	1.0831	.1
2	2.3150	1.4979	1.5068	1.4452	1.4541	2.1383	2.1472	1.2485	1.2467	.1
7	2.3297	1.4166	1.4255	1.2825	1.2914	2.0554	2.0643	1.4932	1.4910	.1
2	2.3532	1.3863	1.3952	1.1513	1.1602	1.9756	1.9845	1.8314	1.8287	.1
8	2.3843	1.4166	1.4255	1.0946	1.1075	1.9033	1.9122	2.2066	2.2035	.1
2	2.4216	1.4979	1.5068	1.1513	1.1602	1.8444	1.8533	2.5000	2.4964	.1
3	2.4638	1.6094	1.6183	1.2825	1.2914	1.8055	1.8144	2.6587	2.6549	.1
9	2.5095	1.7329	1.7418	1.4452	1.4541	1.7918	1.8007	2.7126	2.7088	.1
9	2.5574	1.9568	1.8657	1.6094	1.6183	1.8055	1.8144	2.6961	2.6924	.1
2	2.6067	1.9756	1.9845	1.7632	1.7721	1.8444	1.8533	2.6307	2.6270	.1
2	2.6567	2.0872	2.0961	1.9033	1.9122	1.9033	1.9122	2.5337	2.5302	.1
2	2.7066	2.1910	2.1999	2.0302	2.0391	1.9756	1.9845	2.4212	2.4178	.1
2	2.7561	2.2874	2.2963	2.1452	2.1541	2.0554	2.0643	2.3054	2.3022	.1
2	2.8049	2.3768	2.3857	2.2499	2.2588	2.1383	2.1472	2.1944	2.1913	.1
2	2.8527	2.4600	2.4689	2.3457	2.3546	2.2213	2.2302	2.0921	2.0892	.1
9	2.9006	2.5376	2.5465	2.4338	2.4427	2.3026	2.3115	2.0000	1.9997	.0
2	2.9462	2.6102	2.6191	2.5152	2.5241	2.3811	2.3900	1.9181	1.9177	.0
6	2.9905	2.6783	2.6872	2.5909	2.5998	2.4563	2.4652	1.8457	1.8454	.0
1	3.3644	3.1918	3.1975	3.1439	3.1541	3.0388	3.0490	1.4465	1.4316	1.0
2	3.6387	3.5332	3.5243	3.5006	3.4917	3.4208	3.4119	1.2943	1.2961	-.1
3	3.8610	3.7883	3.7898	3.7636	3.7652	3.7000	3.6939	1.2177	1.2114	.5
2	4.0493	3.9917	3.9843	3.9719	3.9644	3.9192	3.9093	1.1722	1.1733	-.1
2	4.2108	4.1609	4.1610	4.1443	4.1445	4.0993	4.0995	1.1422	1.1363	.5
2	4.3459	4.3055	4.2995	4.2913	4.2853	4.2522	4.2487	1.1210	1.1179	.3
2	4.4674	4.4319	4.4283	4.4195	4.4159	4.3848	4.3799	1.1053	1.1051	.0
1	4.5713	4.5442	4.5359	4.5331	4.5248	4.5020	4.4937	1.0931	1.0928	.0

CHAPTER V

RESULTS AND CONCLUSIONS

The development of this report from the experimental aspect has followed a familiar pattern. The early phases involved familiarization with the technical problems followed by partial success with first attempts at construction. The last phase diverged from the normal course in that data exceeded expected accuracy by such a large margin. The final data indicate that the device is feasible and that it is probably well beyond any commonly available equipment in existence today.

It can be concluded that further effort should be expended to a final product. A design is suggested which is justified as a conservative approach.

As a result of experimental data and consultation with personnel in the semiconductor fabrication industry, there is little doubt that a device for amplitude function takeoff can be constructed. Because of limited facilities, a final unit could not be constructed within the scope of this report. However the problems encountered are such that a theoretical design can be made and simulation performed to prove its applicability.

The proposed mechanical design is illustrated in Figure 18 with the 10 - 1 contact schedule presented in Table I9. The design consists of a 180 to 220 ohms/square wafer with a coating of oxide to prevent deterioration of the surface. The contacts, including the conductive

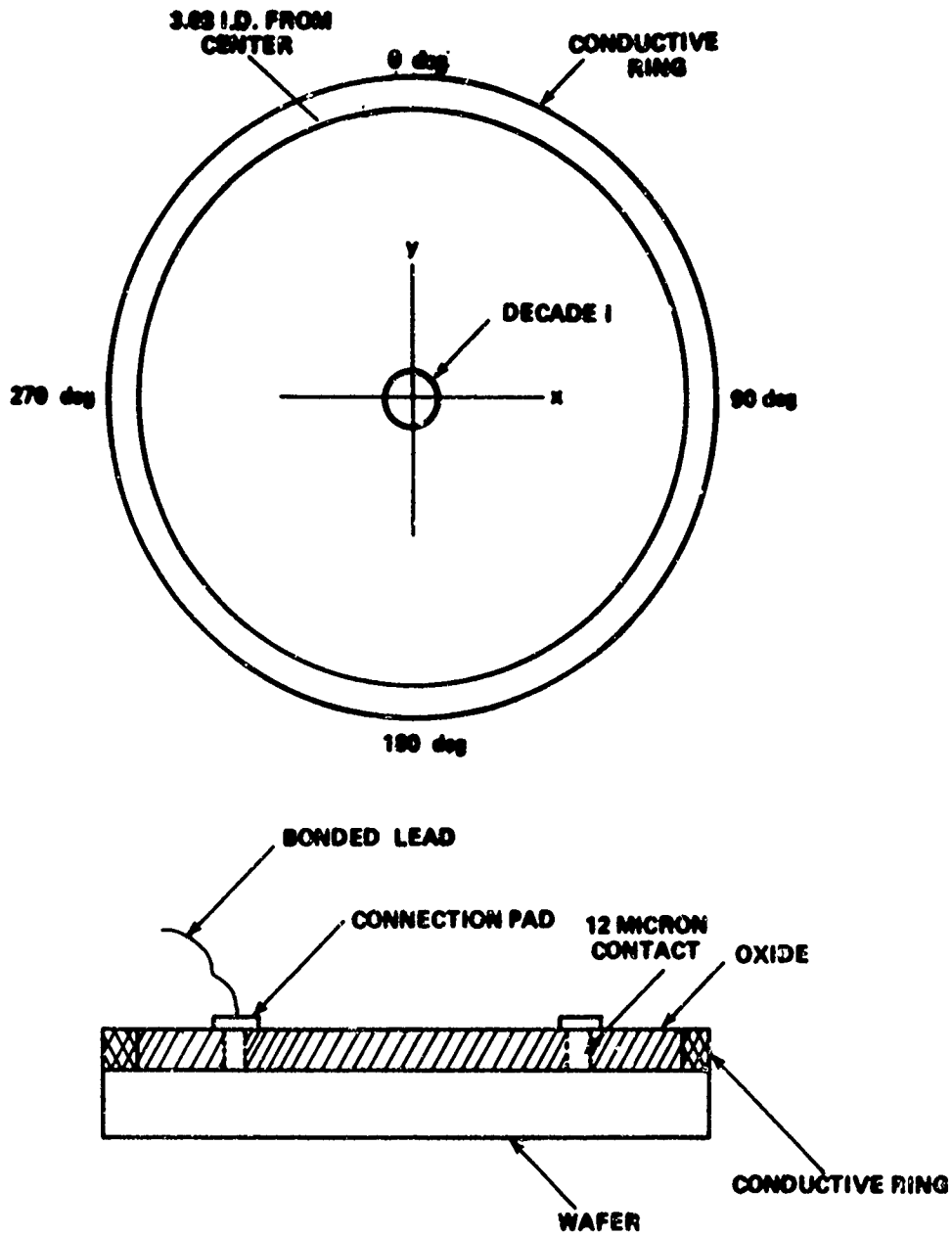


Figure 18. Proposed Laplace function generator wafer design.

Table 19. Wafer design schedule, poles 10 - 1

W	Re 1		Re 10	
	Xin	Yin	Xin	Yin
1	0.015	0	0.15	0
2	-0.015	0.015	-0.15	0.015
3	0.015	-0.030	0.15	-0.030
4	0.015	-0.060	0.15	-0.060
5	-0.015	0.075	-0.15	0.075
6	0.015	-0.090	0.15	-0.090
7	-0.015	0.105	-0.15	0.105
8	0.015	-0.120	0.15	-0.120
9	-0.015	0.135	-0.15	0.135
10	0.015	-0.150	0.15	-0.150
11	-0.015	0.165	-0.15	0.165
12	0.015	-0.180	0.15	-0.180
13	-0.015	0.195	-0.15	0.195
14	0.015	-0.210	0.15	-0.210
15	-0.015	0.225	-0.15	0.225
16	0.015	-0.240	0.15	-0.240
17	-0.015	0.255	-0.15	0.255
18	0.015	-0.270	0.15	-0.270
19	-0.015	0.285	-0.15	0.285
20	0.015	-0.300	0.15	-0.300
30	-0.015	0.450	-0.15	0.450
40	-0.015	-0.600	-0.15	-0.600
50	-0.015	0.750	-0.15	0.750
60	-0.015	-0.900	-0.15	-0.900
70	-0.015	1.05	-0.15	1.05
80	-0.015	-1.20	-0.15	-1.20
90	-0.015	1.35	-0.15	1.35
100	-0.015	-1.50	-0.15	-1.50

ring, are made by penetrating the oxide. This allows use of smaller contacts while the connecting pad can be enlarged above the oxide. A lead is then applied by a bead process to the pad.

It is projected that two real axis poles can be placed on a 3.03-inch wafer, excluding the conductive ring, when arranged in the proper manner.

Then placing two real axis poles, the maximum separation for a near vertical (as apposed to a helix) imaginary axis is obtained by pairing as 10-1, 9-2, 8-3, 7-4, and 6-5.

Data from Chapter IV illustrated that the distortion is within tolerance even with the large pads utilized. Because the distortion is a function of area and displacement, it would appear reasonable that reducing the area factor by 400 would allow for more contacts. It is very likely that a greater number of contacts could be added, thereby reducing the number of wafers required in any given unit. Further experimentation should be conducted to determine the optimum configuration.

In summary experimentation has proven that the amplitude function can be obtained using a thin film semiconductor.

BIBLIOGRAPHY

1. Reynolds, C. C. "Amplitude and Phase Response of Generalized Transfer Functions Utilizing a DC-Analog Laplace Transform Generator." Unpublished Master's thesis, The University of Tennessee, Knoxville, 1971.
2. Huebschmann, E. C., and C. W. Pender. "Simulation of the Laplace Transform by Means of D. C. Potential in Semiconductor Materials." University of Tennessee Space Institute Report DAAH 1-69-C-1735, Tullahoma, Tennessee, September, 1970.
3. Karplus, W. J. Analog Simulation. New York: McGraw-Hill Book Company, Inc., 1958.
4. Kayan, C. E. "An Electrical Geometrical Analogue for Complex Heat Flow," Transactions of the ASME, 67:713-718, November, 1945.
5. Hicks, H., and A. Permoda. "Uniformly Conductive Surfaces," Engineering Research Institute Report AD-20-135, University of Michigan, Ann Arbor, Michigan, September, 1953.
6. Chen, W. H. The Analysis of Linear Systems. New York: McGraw-Hill Book Company, Inc., 1963.
7. Morgan, M. L., and J. C. Looney. "Design of the ESIAC Computer," Quarterly IRE Transactions on Electronic Computers, 10 (Part 3):524-529, September, 1961.